nucleoside antibiotic generated by *Streptomyces* and an inhibitor of N-linked glycosylation and by the formation of *N*-glycosidic protein-carbohydrate linkages.[26] It specifically inhibits dolichol pyrophosphate-mediated glycosylation of asparaginyl residues of glycoproteins,[27] accumulates the unfolded proteins, and induces ER stress.[25,28] To determine the intracellular mechanisms that induce Aβ accumulation in RPE, we treated human retinal pigment epithelial cells, ARPE19 cells, with various ER-stress inducers, such as TM and TG, and investigated the responses of the Aβ accumulation-inducible event.

Materials and Methods

Cell Culture

ARPE19 cells were purchased from the American Type Culture Collection (ATCC, Manassas, VA) and were cultured in Dulbecco modified Eagle medium/F-12 human amniotic membrane nutrient mixture (DMEM/F-12; Sigma-Aldrich, St. Louis, MO) with 10% fetal bovine serum (FBS; Sigma-Aldrich) in a humidified incubator at 37°C in an atmosphere of 5% CO_2. The medium was changed every 3 days.

Preparation of Reagents

TG (Sigma-Aldrich) was dissolved in dimethyl sulfoxide (DMSO; Sigma-Aldrich) at a concentration of 0.5 mM to produce stock solutions. These solutions were diluted to 1:500 with medium to obtain 1 μM TG-containing culture medium. To evaluate the effect of DMSO, medium containing only DMSO (1:500 of total volume) was also prepared for each study. In comparison with TG, 1 μM TM (Sigma-Aldrich) and 0.1 μM staurosporine (STS; Sigma-Aldrich), the bacterial alkaloid that did not induce apoptosis through the ER,[29] were used for each study. Both TG and TM were reported to upregulate *VEGF* mRNA expression in ARPE19 cells.[30] The concentrations of TG and TM used to treat ARPE19 cells were the ones that induced *VEGF* mRNA expression maximally in all experiments in this study. The concentration of STS was selected based on a previous paper.[31] Every reagent was exposed to the ARPE19 cells for 24 hours.

RNA Isolation and cDNA Preparation

Total RNA from ARPE19 cells with exposure to each reagent was isolated (RNA Easy Kit; Qiagen, Tokyo Japan) and quantified by ultraviolet spectrometry at 260 nm. One microgram of RNA was transcribed to cDNA using reverse transcription reagents (Superscript III; Invitrogen, Carlsbad, CA).

Real-Time RT-PCR

Real-time RT-PCR was performed on a thermocycler (7900HT Sequence Detection Systems; Applied Biosystems, Foster, CA) with nuclear stain (SYBR Green; Applied Biosystems) reagents according to the manufacturer's instructions. Amplification of PCR products was measured by fluorescence associated with binding of double-stranded DNA to the SYBR green dye in the reaction mixture. Sequences of the primers used in this study are listed in Table 1. After an initial denaturation step of 50°C for 2 minutes and 95°C for 10 minutes, PCR involved 40 cycles at 95°C for 15 seconds and at 60°C for 1 minute. Quantification of each PCR product was expressed relative to GAPDH.

RT-PCR

For semiquantitative experiments, each PCR amplification was tested to reach half the saturation curve, and an aliquot of cDNA libraries was amplified by PCR with specific oligonucleotides for *APP* isoforms *APP770*, *APP751*, and *APP695* (605, 586, and 418 bp, respectively, of PCR product). APP primers were designed to flank the alternatively spliced exons (exons 7 and 8) to detect the expression of the three major APP isoforms found in the brain. Oligonucleotide sequences used were as follows: sense, 5′-aga gag aac cac cag cat tgc c-3′ (992–1013 bp); antisense, 5′-ggt cat tga gca tgg ctt cca c-3′ (1575–1596). These sequences were designed from the human APP cDNA sequences corresponding to GenBank accession number NM_000484. Amplification was performed in a thermocycler (PCR System 9700; Applied Biosystems). Conditions of amplification were 30 seconds at 95°C, 30 seconds at 57°C, and 1 minute at 72°C for 28 cycles to detect *APP770* and *APP751* or for 33 cycles to detect *APP695*. Finally, 5% polyacrylamide gels were stained by ethidium bromide and acquired with a CCD camera. mRNA levels were quantified using NIH image and normalized to the GAPDH levels.

Western Blot

Cells were homogenized in lysis buffer (10 mM Tris-HCl [pH 8.0], 1 mM EDTA, 150 mM NaCl, 0.5% NP-40) and were stored in sample buffer (50 mM TBS containing 2% sodium dodecyl sulfate [SDS], 6% β-mercaptoethanol, 10% glycerol) at −20°C until use. Quantification of the protein contents was made by the Bradford method.

Protein samples (15 μg) were separated on SDS-PAGE (12% acrylamide) and were transferred to polyvinylidene difluoride filters (Millipore, Bedford, MA). The filters were blocked in 0.1 M PBS containing 5% skim milk and 0.05% Tween 20 for 1 hour at room temperature and were incubated overnight at 4°C with a monoclonal mouse anti-

Table 1. Primer Sequences Used in This Study

Gene	Oligo Name	Sequence	Accession No.
APP	Forward	ctg gcc ctg gag aac tac atc a	NM_000484
	Reverse	gcg cgg aca tac ttc ttt agc a	
BACE	Forward	tca ccc aag gtc acc aaa caa c	NM_012104
	Reverse	tga agt cct cac cct ttc cca t	
caspase-4	Forward	ctg aag gac aaa ccc aag gtc a	U25804
	Reverse	cac ttc caa gga tgc tgg aga g	
ECE	Forward	aac tcc aac agc aac gtg atc c	NM_001397
	Reverse	cgg tca gca cct tct cgt ttt	
GAPDH	Forward	cac tga atc tcc cct cct cac a	NM_002046
	Reverse	tga tgg tac atg aca agg tgc g	
neprilysin	Forward	cat cgg cat ggt cat agg aca	NM_007287
	Reverse	tgt tga gtc cac cag tca acg a	
PEDF	Forward	gcc agg tcc aca aag gaa att	AF_400442
	Reverse	aac ttt gtt acc cac tgc ccc	
TACE	Forward	ttc act gga cac gtg gtt ggt	NM_002046
	Reverse	ggc ccc atc tgt gtt gat tct	
TNF-α	Forward	aac aac cct cag acg cca cat	NM_000594
	Reverse	cag tgc tca tgg tgt cct ttc c	
VEGF	Forward	aag aag cag ccc atg aca gct	NM_001025366
	Reverse	tag gtc ctt tta ggc tgc acc c	

caspase-4 (1:1000; MBL, Nagano Japan) and a polyclonal rabbit anti-VEGF (1:200; Santa Cruz Biotechnology, Santa Cruz, CA) primary antibody. After five washes in 0.1 M PBS containing 0.05% Tween 20, the filters were incubated for 1 hour at room temperature with a horseradish peroxidase (HRP)-conjugated anti-mouse IgG (1:1000; Cell Signaling, Beverly, MA) and an anti-rabbit IgG (1:1000; Cell Signaling) secondary antibody, washed, visualized in ECL solution (Amersham Biosciences, Arlington Heights, IL) for 10 minutes, and exposed onto film (X-Omat; Fuji, Kanagawa, Japan) for 7 to 10 minutes. Finally, the filters were incubated in a stripping buffer (2% SDS, 0.7% β-mercaptoethanol, 62.5 mM Tris-HCl, pH 6.8) for 30 minutes at 65°C and were reprobed with a monoclonal mouse anti-β-actin antibody (1:3000; Chemicon, Temecula, CA) as loading controls. Our Western blot bands showed the same band sizes as indicated in the antibody information sheets. Protein levels were quantified by densitometry and normalized to the β-actin levels.

Data and Statistical Analyses

Statistical analysis of mRNA and protein expression levels for each reagent treatment was performed using the Student's *t*-test in comparisons with DMSO treatment (control). Data were expressed as mean ± SE ($n = 3$).

Intracellular Ca^{2+} Measurement

The intracellular Ca^{2+} concentration in retinal pigment epithelial cells was monitored using the Ca^{2+} indicator dye (Fluo-4; Invitrogen). After 3 days in vitro, cells were incubated for 20 minutes with the cell-permeant acetomethyl ester form of 5 mM Ca^{2+} indicator dye (Fluo-4; Invitrogen) diluted in culture medium containing 0.01% pluonic acid F-127 at 37°C. The cells were subsequently washed three times with culture medium, and the dye was allowed to deesterify for an additional 30 minutes in the CO_2 incubator. Ca^{2+} imaging experiments were performed using a live cell imaging microscope system (BioStation IM; Nikon, Tokyo, Japan) with a 20× objective. Fluorescent images were acquired every 20 seconds. Fluo-4 fluorescence was produced by excitation from a 130-W mercury-vapor lamp and an appropriate filter set (B-2A [Nikon]; excitation, 450–490 nm; emission, 520–560 nm; dichroic, 510 nm). All drugs were applied by bath application after 5-minute control observation. Data analysis was performed as follows: off-line analysis of the images was performed using commercial software (Aquacosmos; Hamamatsu Photonics, Hamamatsu, Japan). Fluorescence signal was quantified by measuring the average pixel intensity within cell bodies. Changes in fluorescence intensity of each cell were normalized to its baseline fluorescence intensity.

Results

Induction of Aβ Production-Inducible APP Splice Variants mRNA Expression in ER-Stress–Treated ARPE19 Cells

In the amyloidogenic pathway, the cleavage of APP by the β-secretase and presenilin complex results in Aβ production. *APP* has several splice variants. Exons 7, 8, and 15 of the *APP* gene can be alternatively spliced to produce multiple isoforms. In the brain, the major isoform transcripts result from the splicing of exons 7 and 8, which gives rise to APP695, APP751, and APP770.[20] Both APP770 and APP751 contain a serine protease inhibitory domain encoded by exon 7 called the Kunitz protease inhibitory domain (KPI). KPI-APP has been shown to be more amyloidogenic than KPI-deficient APP.[32]

In the ARPE19 cells, the exposure of TG, which induces a depletion of intracellular Ca stores, slightly increased the expression of *KPI-APP*, such as *APP751* and *APP770* (Fig. 1A). TM, which inhibits N-linked glycosylation, induced an increase of *KPI-APP* expression in ARPE19 cells (Fig. 1A). STS, which is widely used as an inducer of non-ER stress-induced apoptosis, did not induce the expression of *KPI-APP* (Fig. 1A). Real-time RT-PCR showed no change in the total *APP* mRNA expression of any of the reagent treatments (Fig. 1B). These results indicate that ER stress induces mRNA expression of *APP* splice variants, which accelerate Aβ accumulation, in ARPE19 cells.

Decrease of Aβ Metabolism-Related Factors mRNA Expression in TG-Treated ARPE19 Cells

To find the relationship between ER stress-inducing factors and cellular mRNA expression of a series of Aβ metabolism-related factors (such as neprilysin, ECE, and BACE) in ARPE19 cells, we performed real-time RT-PCR.

TG-treated ARPE19 cells showed a remarkable decrease in mRNA expression of neprilysin, which highly degrades $A\beta^{33-34}$ (Fig. 2A). The mRNA expression of *ECE*, which degrades Aβ, and of *BACE*, which cleaves APP at the β site, was not quantitatively changed by TG (Figs. 2B, 2C). The expression of all investigated Aβ metabolism-related genes were not affected by TM or STS treatment (Fig. 2). Because there was a remarkable

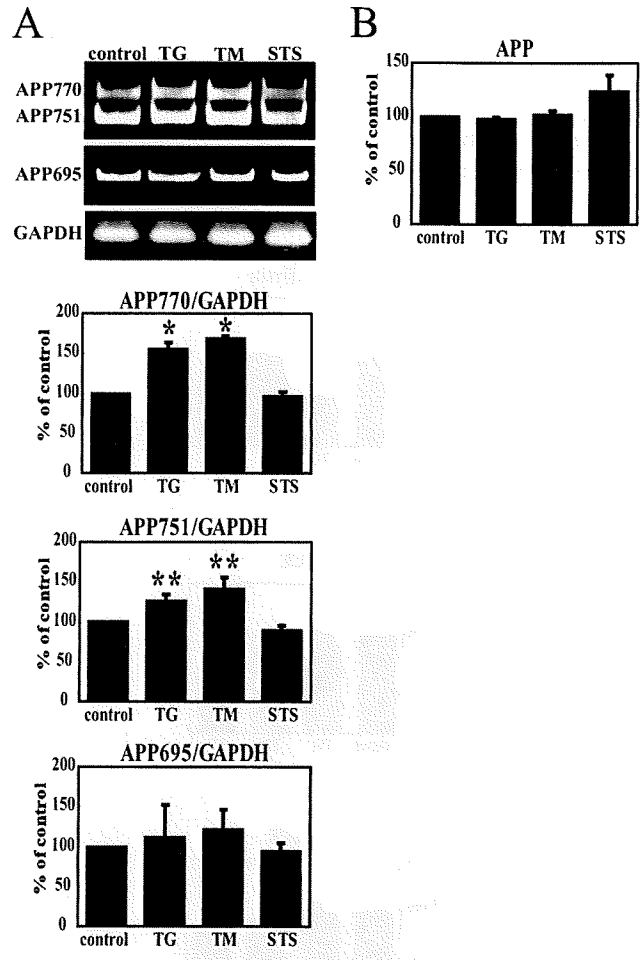

FIGURE 1. (A) Transcriptional expression of APP isoforms in cultured ARPE19 cells induced by TG, TM, and STS by RT-PCR analysis and densitometric analyses. Data are expressed as the mean ± SE ($n = 3$). The results show that TG and TM treatment induced a slight increase in *APP751* and *APP770* but not *APP695* compared with the control. $^{**}P < 0.05$ and $^{*}P < 0.01$ for comparison with the control, by Student's *t*-test. (B) Expression of *APP* mRNA induced by TG, TM, and STS using real-time RT-PCR analysis. Data are expressed as mean ± SE ($n = 3$). Expression of *APP* did not change in all ARPE19 cell samples compared with the control. $^{*}P < 0.01$ for comparison with the control, by Student's *t*-test.

decrease of neprilysin mRNA observed in only TG-treated cells, it is suggested that the degradation of Aβ is depressed by a decrease in the expression of neprilysin in ARPE19 cells.

Induction of Angiogenic Factors mRNA Expression in ER-Stress–Treated ARPE19 Cells

It has been reported that exposure to Aβ induced the mRNA expression of *VEGF* and a reduction of *PEDF* in ARPE19 cells.[12] We investigated the cellular mRNA expression change of *VEGF* and *PEDF* produced by TG and TM treatment in ARPE19 cells. In addition, real-time RT-PCR was performed for tumor necrosis factor alpha (*TNF-α*) and TNF-α converting enzyme (*TACE*). TNF-α, a macrophage/monocyte-derived polypeptide, stimulates VEGF production in human glioma cells and retinal pigment epithelial cells,[35,36] and TACE is involved the generation of soluble TNF-α from membrane-bound TNF-α and promotes angiogenesis.[37,38]

TG and TM exclusively upregulated *VEGF* mRNA expression, as reported previously,[30] as did STS (Fig. 3A). Real-time RT-PCR showed that TG and STS exclusively downregulated *PEDF* mRNA expression, and TM did not change (Fig. 3B). TG and TM also upregulated the mRNA expression of *TNF-α* and *TACE* (Figs. 3C, 3D). STS upregulated the mRNA expression of *TNF-α* but did not change that of *TACE* (Figs. 3C, 3D). To confirm the increase of VEGF expression at the protein level, we performed Western blot analysis for VEGF and showed that TG and TM also upregulated VEGF protein expression (Fig. 3E). These results suggest that the change in expression of these angiogenic factors might be the result of a general apoptotic event.

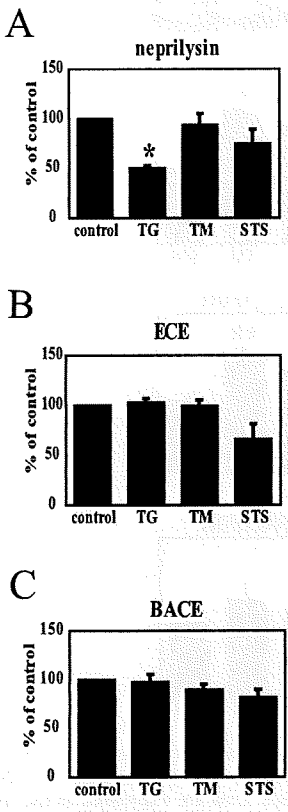

FIGURE 2. Expression of Aβ-metabolic process-related genes such as neprilysin (**A**), *ECE* (**B**), and *BACE* (**C**) mRNA induced by TG, TM, and STS using real-time RT-PCR analysis. Data are expressed as mean ± SE ($n = 3$). Expression of *ECE* (**B**) and *BACE* (**C**) did not change in all ARPE19 cells sample compared with the control. Expression of neprilysin (**A**) mRNA decreased in only TG-treated ARPE19 cells compared with the control. $^*P < 0.01$ for comparison with the control, by Student's *t*-test.

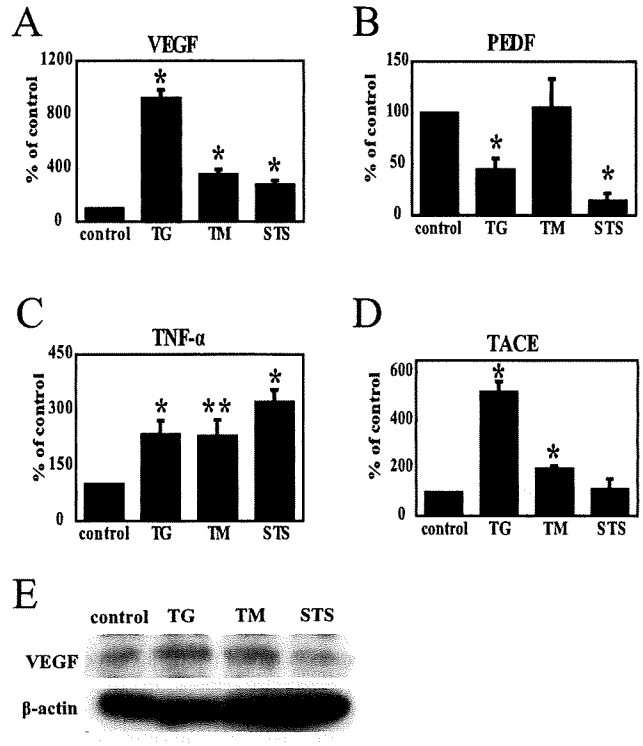

FIGURE 3. Expression of angiogenesis-related genes such as *VEGF* (**A**), *PEDF* (**B**), *TNF-α* (**C**), and *TACE* (**D**) induced by TG, TM, and STS using real-time RT-PCR analysis. Data are expressed as mean ± SE ($n = 3$). Graphs show the upregulation of *VEGF* (**A**), *TNF-α* (**C**), and mRNA in all ARPE19 cell samples compared with the control. Expression of *PEDF* (**B**) decreased in TG- and STS-induced ARPE19 cell mRNA compared with the control. Expression of *TACE* (**D**) increased in TG- and TM-induced ARPE19 cell mRNA compared with the control. $^{**}P < 0.05$ and $^*P < 0.01$ for comparison with the control, by Student's *t*-test (**E**) Expression of VEGF protein induced by TG, TM, and STS using Western blot. Results show the upregulation of VEGF as it was affected by TG and TM compared with the control. These data were confirmed by three independent Western blot analyses.

Induction of Caspase-4 Expression in TG-Treated ARPE19 Cells

Caspase-4 is primarily activated in ER stress-induced apoptosis.[39] Real-time RT-PCR and Western blot showed that the expression of caspase-4 mRNA and the active form of its protein were upregulated by TG treatment (Fig. 4). Although expression of the active form of caspase-4 protein was also upregulated by TM treatment, it was much lower than that of TG-treated ARPE19 cells (Fig. 4). STS-treated ARPE19 cells showed no change in expression of caspase-4 (Fig. 4).

Induction of Intracellular Ca Elevation in TG-Treated ARPE19 Cells

TG can inhibit the sarcoplasmic reticulum calcium-ATPase and can elevate intracellular Ca concentration.[23] We performed Ca imaging (Fluo-4 and Fura-2/AM; Invitrogen) to investigate whether the intracellular Ca concentration was actually increased in TG-treated ARPE19 cells. TG-treated ARPE19 cells showed a remarkable increase in intracellular Ca concentration (Fig. 5 and Supplementary Fig. S1, online at http://www.iovs.org/cgi/content/full/49/6/2376/DC1). TM- and STS-treated

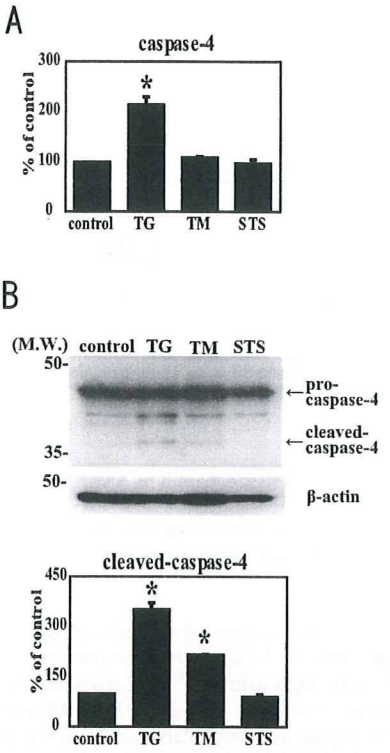

FIGURE 4. (A) Expression of caspase-4 induced by TG, TM, and STS using real-time RT-PCR analysis. The graph shows the upregulation of caspase-4 mRNA as it was affected by TG compared with the control. (B) Expression of the active-form of caspase-4 (cleaved-caspase-4) induced by TG, TM, and STS using Western blot and densitometric analyses. Results show the activation of caspase-4 as it was affected by TG and TM compared with the control. Data are expressed as mean ± SE ($n = 3$). $^*P < 0.01$ for comparison with the control, by Student's t-test.

ARPE19 cells showed no change in intracellular Ca concentration (Fig. 5 and Supplementary Fig. S1).

DISCUSSION

Recently, it has been reported that Aβ accumulates in the RPE of patients with AMD,[3–5] which is the most common cause of vision loss in the development of CNV. Aβ, known as the hallmark of AD, is routinely produced in the normal brain and is readily degraded by catabolic enzymes. However, facilitation of Aβ production is caused by mutation of the gene responsible for AD. Aβ then accumulates as the insoluble senile plaques in the brain. ER stress is considered one of the causative factors for the accumulation of Aβ in AD.[10] To examine the intracellular machinery for Aβ accumulation in the RPE of patients with AMD, we treated human retinal pigment epithelial cells, ARPE19 cells, with the ER-stress inducer and investigated whether Aβ accumulation was inducible. Our results suggested that Aβ accumulation-inducible factors were induced by ER stress in retinal pigment epithelial cells as well as in neural cells, and angiogenic factors were additively increased in retinal pigment epithelial cells by ER stress under the same conditions.

We showed that ER stress treatment induced an increase in mRNA expression of Aβ production-inducible *APP* splice variants; only TG treatment further induced a decrease in the mRNA expression of neprilysin in ARPE19 cells (Figs. 1, 2). It has been reported that KPI-APP, which increases at the mRNA level in the brains of persons with AD,[11] is more amyloidogenic than KPI-deficient APP.[32] Therefore, it is thought that the increase in mRNA expression of KPI-APP induced the production of Aβ. On the other hand, neprilysin knockout mice have been reported to display an approximately 50% increase in the levels of Aβ40 and Aβ42.[14] Based on these facts, we surmised that the increased Aβ production and the decreased Aβ degradation induced specifically by TG treatment in ARPE19 cells might be attributed to the Aβ accumulation in ARPE19 cells.

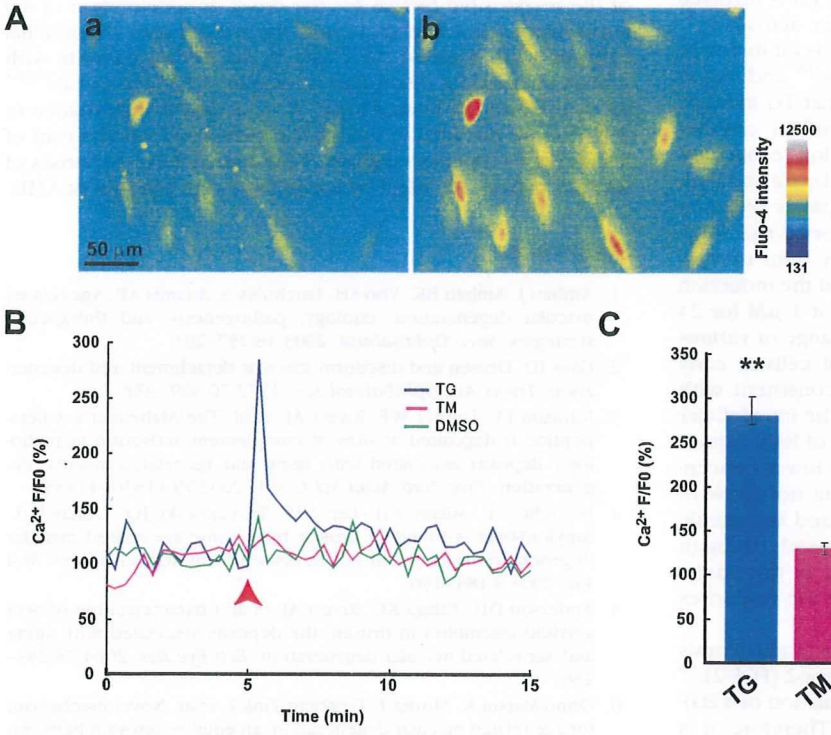

FIGURE 5. Effects of TG and TM on Ca^{2+} elevation in retinal pigment epithelial cell soma. (A) A representative experiment showing that TG (1 μM) evoked increases in cytosolic Ca^{2+}. These images are pseudocolor images of Ca^{2+} indicator dye fluorescence (a, 0 min; b, 20 seconds after TG application). Scale bar, 50 mm. (B) Representative traces showing the average changes in Ca^{2+} indicator dye fluorescence of the retinal pigment epithelial cells. Spontaneous Ca^{2+} elevations were also observed in retinal pigment epithelial cells before the application of drugs. Note that the application of TG rapidly and markedly increased Ca^{2+} indicator dye fluorescence. (C) Average amplitudes of first peaks after drug application. Note that TG significantly increased the peak amplitude of Ca^{2+} elevation but that TM did not. Statistical differences were established using the Mann-Whitney U test at $^{**}P < 0.01$ ($n = 34$–58). Error bars indicate SEMs.

We also confirmed that the upregulation of *TNF-α*, *TACE*, and *VEGF* and the downregulation of *PEDF* were induced by TG treatment in ARPE19 cells at the mRNA level (Figs. 3A–D). Moreover, VEGF protein expression was upregulated by TG treatment (Fig. 3E), suggesting that TG treatment induced the expression not only of Aβ accumulation-promoting factor expression but also of angiogenic factors in ARPE19 cells.

Because transcription factor 4, activated by ER stress, induced VEGF,[42] ER stress has been considered to induce not only Aβ accumulation but also angiogenesis. However, our results showed a pronounced difference in the responses of Aβ accumulation-promoting factors and angiogenic factors between TG and TM, likely because of two reasons. First, there was a difference in the extent of ER stress-induced apoptosis. Caspase-4, which is primarily activated in ER stress-induced apoptosis,[39] was shown to be activated in TG-treated ARPE19 cells more than in TM-treated ARPE19 cells (Fig. 4). Second, we conjectured that the difference in results was attributed to the mechanism of action of each ER stress inducer. TG-induced ER stress was caused by the depletion of intracellular Ca stores,[24] whereas TM-induced ER stress was caused by an inhibition of N-linked glycosylation.[28] Differing from both TM- and STS-treated ARPE19 cells, we showed TG-treated ARPE19 cell exhibited striking increases in intracellular Ca concentration. It has been reported that insulin-like growth factor-1 stimulates increased VEGF secretion through the induction of the second messenger Ca in ARPE19 cells.[43] The elevation of intracellular Ca levels was also reported to increase Aβ peptide production through the activation of a protease, which requires Ca, in the cultured cells.[44] Based on these facts, intracellular increases of Ca by TG treatment may induce Aβ accumulation and angiogenic factors in ARPE19 cells more effectively than ER stress induced by TM.

It has long been known that the elevation of intracellular free calcium by TG has cytotoxic consequence in many cells (adipocytes,[45] T lymphocytes,[46] parotid acinar cells,[47] and peritoneal macrophages[48]) and cell lines (hepatocytes,[49] HeLa cells,[50] and NG115-401L cells[24]), including ARPE19 cells.[51] TM was used mainly for analysis in N-glycosylation (except that TM was used as an ER-stress inducer), whereas TG is involved in various cellular functions, including platelet activation,[52] inflammation,[53] skin irritation,[54] protein synthesis inhibition in human hepatoma cells,[55] vascular contractility,[56] and tumor promotion.[55] Moreover, it has been reported that TG induced Bax activation and was involved in mitochondrial caspase-dependent death.[57] It was often said that the low concentrations (0.5–2 μM) of TG increased the intracellular Ca and high concentration (1–10 μM) of TG-induced apoptosis (refer to Sigma data sheet). In addition, it has been reported that long-term (48-hour) exposure of TG led to recovery from upregulation of the intracellular Ca concentration[58] and the induction of cell death.[49] In our study, TG was exposed at 1 μM for 24 hours because we wanted to determine the change of various factors in the viable retinal pigment epithelial cells at early stages of Aβ accumulation. Our results were consistent with those of a previous report[51] in the elevation of the intracellular Ca concentration (Fig. 5). However, the change of BAX expression was not induced, probably because of the lower concentration and shorter incubation time of TG (data not shown). Therefore, TG would induce Aβ accumulation and angiogenic responses in retinal pigment epithelial cells mainly through induction of the intracellular Ca concentration in this study. Further studies would be needed to determine the responses under various conditions of TG incubation.

It has been reported that neprilysin inhibits angiogenesis through the proteolysis of fibroblast growth factor-2 (FGF-2),[59] and neprilysin knockout mice display an upregulation of VEGF and a downregulation of PEDF in their RPE.[12] Therefore, it is possible that the reduction of neprilysin mRNA expression induces angiogenesis. VEGF, which increases in AD patients, binds to Aβ with high affinity,[60] and Aβ stimulates the angiogenic response through FGF-2.[61] In addition, Aβ-treated ARPE19 cells display an upregulation of VEGF and a downregulation of PEDF.[12] Taken together, these reports suggest the possibility that Aβ induces angiogenesis. However, in our study, it was unclear whether Aβ or neprilysin directly affected angiogenesis because the stress-inducer treatment time was short.

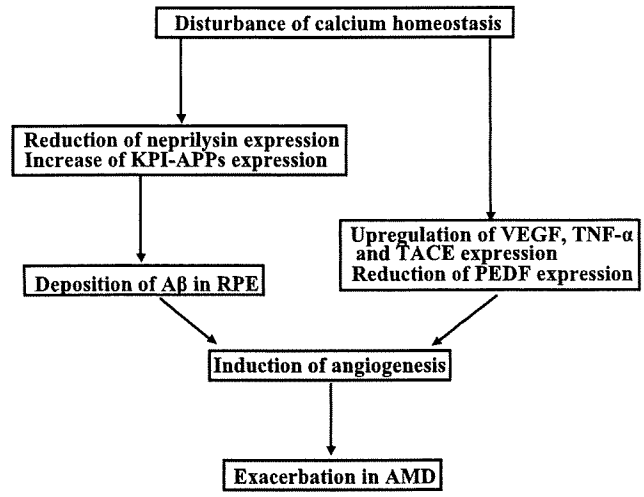

FIGURE 6. Display of the hypothesis that the disturbances in Ca homeostasis involve the pathogenic mechanism of AMD.

In the present study, we demonstrated that ER stress could cause the promotion of Aβ accumulation-inducible and angiogenic factors at the mRNA level in ARPE19 cells. Moreover, we showed that TG induced those factors more effectively than TM. Therefore, we propose that TG treatment produced an elevation of the intracellular Ca concentration, which was one of the responsible factors for the onset or acceleration of Aβ accumulation and angiogenesis in the retinal pigment epithelial cultured cells. Because Aβ exists in the RPE of patients with AMD and caused a disruption of cellular Ca homeostasis,[62,63] we speculate that intracellular Ca homeostasis disturbance in RPE may be involved in one of the pathogenic mechanism of AMD (Fig. 6). Detailed analysis of the intracellular responses of ARPE19 cells to TG might be useful for the mechanism of AMD.

References

1. Ambati J, Ambati BK, Yoo SH, Ianchulev S, Adamis AP. Age-related macular degeneration: etiology, pathogenesis, and therapeutic strategies. *Surv Ophthalmol.* 2003;48:257–293.
2. Gass JD. Drusen and disciform macular detachment and degeneration. *Trans Am Ophthalmol Soc.* 1972;70:409–436.
3. Johnson LV, Leitner WP, Rivest AJ, et al. The Alzheimer's A beta-peptide is deposited at sites of complement activation in pathologic deposits associated with aging and age-related macular degeneration. *Proc Natl Acad Sci U S A.* 2002;99:11830–11835.
4. Dentchev T, Milam AH, Lee VM, Trojanowski JQ, Dunaief JL. Amyloid-beta is found in drusen from some age-related macular degeneration retinas, but not in drusen from normal retinas. *Mol Vis.* 2003;9:184–190.
5. Anderson DH, Talaga KC, Rivest AJ, et al. Characterization of beta amyloid assemblies in drusen: the deposits associated with aging and age-related macular degeneration. *Exp Eye Res.* 2004;78:243–256.
6. Ohno-Matsui K, Morita I, Tombran-Tink J, et al. Novel mechanism for age-related macular degeneration: an equilibrium shift between

the angiogenesis factors VEGF and PEDF. *J Cell Physiol.* 2001;189:323-333.
7. Duh EJ, Yang HS, Haller JA, et al. Vitreous levels of pigment epithelium-derived factor and vascular endothelial growth factor: implications for ocular angiogenesis. *Am J Ophthalmol.* 2004;137:668-674.
8. Campochiaro PA, Hackett SF. Ocular neovascularization: a valuable model system. *Oncogene.* 2003;22:6537-6548.
9. Witmer AN, Vrensen GF, Van Noorden CJ, Schlingemann RO. Vascular endothelial growth factors and angiogenesis in eye disease. *Prog Retin Eye Res.* 2003;22:1-29.
10. Dawson DW, Volpert OV, Gillis P, et al. Pigment epithelium-derived factor: a potent inhibitor of angiogenesis. *Science.* 1999;285:245-248.
11. Tombran-Tink J, Shivaram SM, Chader GJ, Johnson LV, Bok D. Expression, secretion, and age-related downregulation of pigment epithelium-derived factor, a serpin with neurotrophic activity. *J Neurosci.* 1995;15:4992-5003.
12. Yoshida T, Ohno-Matsui K, Ichinose S, et al. The potential role of amyloid beta in the pathogenesis of age-related macular degeneration. *J Clin Invest.* 2005;115:2793-2800.
13. Saido TC. Alzheimer's disease as proteolytic disorders: anabolism and catabolism of beta-amyloid. *Neurobiol Aging.* 1998;19:S69-S75.
14. Iwata N, Tsubuki S, Takaki Y, et al. Metabolic regulation of brain Aβ by neprilysin. *Science.* 2001;292:1550-1552.
15. Selkoe DJ. Alzheimer's disease: genes, proteins, and therapy. *Physiol Rev.* 2001;81:741-766.
16. Vassar R, Bennett BD, Babu-Khan S, et al. Beta-secretase cleavage of Alzheimer's amyloid precursor protein by the transmembrane aspartic protease BACE. *Science.* 1999;286:735-741.
17. Takasugi N, Tomita T, Hayashi I, et al. The role of presenilin cofactors in the gamma-secretase complex. *Nature.* 2003;422:438-441.
18. Iwata N, Takaki Y, Fukami S, Tsubuki S, Saido TC. Region-specific reduction of A beta-degrading endopeptidase, neprilysin, in mouse hippocampus upon aging. *J Neurosci Res.* 2002;70:493-500.
19. Eckman EA, Reed DK, Eckman CB. Degradation of the Alzheimer's amyloid beta peptide by endothelin-converting enzyme. *J Biol Chem.* 2001;276:24540-24548.
20. Selkoe DJ. Amyloid beta-protein and the genetics of Alzheimer's disease. *J Biol Chem.* 1996;271:18295-18298.
21. Wong WL, Brostrom MA, Kuznetsov G, Gmitter-Yellen D, Brostrom CO. Inhibition of protein synthesis and early protein processing by thapsigargin in cultured cells. *Biochem J.* 1993;289(pt 1):71-79.
22. Sato N, Imaizumi K, Tohyama M, et al. Increased production of β-amyloid and vulnerability to endoplasmic reticulum stress by an aberrant spliced form of presenilin 2. *J Biol Chem.* 2001;276:2108-2114.
23. Treiman M, Caspersen C, Christensen SB. A tool coming of age: thapsigargin as an inhibitor of sarco-endoplasmic reticulum Ca^{2+}-ATPases. *Trends Pharmacol Sci.* 1998;19:131-135.
24. Jackson TR, Patterson SI, Thastrup O, Hanley MR. A novel tumour promoter, thapsigargin, transiently increases cytoplasmic free Ca^{2+} without generation of inositol phosphates in NG115-401L neuronal cells. *Biochem J.* 1988;253:81-86.
25. Lee AS. The glucose-regulated proteins: stress induction and clinical applications. *Trends Biochem Sci.* 2001;26:504-510.
26. Mahoney WC, Duksin D. Biological activities of the two major components of tunicamycin. *J Biol Chem.* 1979;254:6572-6576.
27. Olden K, Pratt RM, Jaworski C, Yamada KM. Evidence for role of glycoprotein carbohydrates in membrane transport: specific inhibition by tunicamycin. *Proc Natl Acad Sci U S A.* 1979;76:791-795.
28. Patil C, Walter P. Intracellular signaling from the endoplasmic reticulum to the nucleus: the unfolded protein response in yeast and mammals. *Curr Opin Cell Biol.* 2001;13:349-355.
29. Mao YW, Liu JP, Xiang H, Li DW. Human αA- and αB-crystallins bind to Bax and Bcl-X(S) to sequester their translocation during staurosporine-induced apoptosis. *Cell Death Differ.* 2004;11:512-526.
30. Abcouwer SF, Marjon PL, Loper RK, Vander, Jagt DL. Response of VEGF expression to amino acid deprivation and inducers of endoplasmic reticulum stress. *Invest Ophthalmol Vis Sci.* 2002;43:2791-2798.
31. John PM, Neville NO. Induction of apoptosis in cultured human retinal pigmented epithelial cells the effect of protein kinase c activation and inhibition. *Neurochem Int.* 1997;31:261-273.
32. Ho L, Fukuchi K, Younkin SG. The alternatively spliced Kunitz protease inhibitor domain alters amyloid beta protein precursor processing and amyloid beta protein production in cultured cells. *J Biol Chem.* 1996;271:30929-30934.
33. Shirotani K, Tsubuki S, Iwata N, et al. Neprilysin degrades both amyloid beta peptides 1-40 and 1-42 most rapidly and efficiently among thiorphan- and phosphoramidon-sensitive endopeptidases. *J Biol Chem.* 2001;276:21895-21901.
34. Takaki Y, Iwata N, Tsubuki S, et al. Biochemical identification of the neutral endopeptidase family member responsible for the catabolism of amyloid beta peptide in the brain. *J Biochem (Tokyo).* 2000;128:897-902.
35. Ryuto M, Ono M, Izumi H, et al. Induction of vascular endothelial growth factor by tumor necrosis factor alpha in human glioma cells: possible roles of SP-1. *J Biol Chem.* 1996;271:28220-28228.
36. Oh H, Takagi H, Takagi C, et al. The potential angiogenic role of macrophages in the formation of choroidal neovascular membranes. *Invest Ophthalmol Vis Sci.* 1999;40:1891-1898.
37. Black RA, Rauch CT, Kozlosky CJ, et al. A metalloproteinase disintegrin that releases tumour-necrosis factor-alpha from cells. *Nature.* 1997;385:729-733.
38. Moss ML, Jin SL, Milla ME, et al. Cloning of a disintegrin metalloproteinase that processes precursor tumour-necrosis factor-alpha. *Nature.* 1997;385:733-736.
39. Hitomi J, Katayama T, Eguchi Y, et al. Involvement of caspase-4 in endoplasmic reticulum stress-induced apoptosis and Aβ-induced cell death. *J Cell Biol.* 2004;165:347-356.
40. Katayama T, Imaizumi K, Manabe T, et al. Induction of neuronal death by ER stress in Alzheimer's disease. *J Chem Neuroanat.* 2004;28:67-78.
41. Preece P, Virley DJ, Constandi M, et al. Amyloid precursor protein mRNA levels in Alzheimer's disease brain. *Brain Res Mol Brain Res.* 2004;122:1-9.
42. Ameri K, Harris AL. Activating transcription factor 4. *Int J Biochem Cell Biol.* 2008;40:14-21.
43. Rosenthal R, Wohlleben H, Malek G, et al. Insulin-like growth factor-1 contributes to neovascularization in age-related macular degeneration. *Biochem Biophys Res Commun.* 2004;323:1203-1208.
44. Querfurth HW, Selkoe DJ. Calcium ionophore increases amyloid beta peptide production by cultured cells. *Biochemistry.* 1994;33:4550-4561.
45. Begum N, Leitner W, Reusch JE, Sussman KE, Drazninz B. GLUT-4 phosphorylation and its intrinsic activity: mechanism of Ca(2+)-induced inhibition of insulin-stimulated glucose transport. *J Biol Chem.* 1993;268:3352-3356.
46. Gouy H, Cefai D, Christensen SB, Debre P, Bismuth G. Ca^{2+} influx in human T lymphocytes is induced independently of inositol phosphate production by mobilization of intracellular Ca^{2+} stores: a study with the Ca^{2+} endoplasmic reticulum-ATPase inhibitor thapsigargin. *Eur J Immunol.* 1990;20:2269-2275.
47. Takemura H, Hughes AR, Thastrup O, Putney JW Jr. Activation of calcium entry by the tumor promoter thapsigargin in parotid acinar cells. *J Biol Chem.* 1989;264:12266-12271.
48. Ohuchi K, Sugawara T, Watanabe M, et al. Analysis of the stimulative effect of thapsigargin, a non-TPA-type tumour promoter, on arachidonic acid metabolism in rat peritoneal macrophages. *Br J Pharmacol.* 1988;94:917-923.
49. Canova NK, Kmonickova E, Martinek J, Zidek Z, Farghali H. Thapsigargin, a selective inhibitor of sarco-endoplasmic reticulum Ca 2-ATPases, modulates nitric oxide production and cell death of primary rat hepatocytes in culture. *Cell Biol Toxicol.* 2007;23:337-354.
50. Middleton JP, Albers FJ, Dennis VW, Raymond JR. Thapsigargin demonstrates calcium-dependent regulation of phosphate uptake in HeLa cells *Am J Physiol.* 1990;259:F727-F731.

51. Reigada D, Lu W, Zhang X, et al. Degradation of extracellular ATP by the retinal pigment epithelium. *Am J Physiol Cell Physiol.* 2005;289:617-624.
52. Thastrup O, Linnebjerg H, Bjerrum PJ, Knudsen JB, Christensen SB. The inflammatory and tumor-promoting sesquiterpene lactone, thapsigargin, activates platelets by selective mobilization of calcium as shown by protein phosphorylations. *Biochim Biophys Acta.* 1987;927:65-73.
53. Ali H, Christensen SB, Foreman JC, et al. The ability of thapsigargin and thapsigargicin to activate cells involved in the inflammatory response. *Br J Pharmacol.* 1985;85:705-712.
54. Hakii H, Fujiki H, Suganuma M, et al. Thapsigargin, a histamine secretagogue, is a non-12-O-tetradecanoylphorbol-13-acetate (TPA) type tumor promoter in two-stage mouse skin carcinogenesis. *J Cancer Res Clin Oncol,* 1986;111:177-181.
55. Wong WL, Brostrom MA, Kuznetsov G, Gmitter-Yellen D, Brostrom CO. Inhibition of protein synthesis and early protein processing by thapsigargin in cultured cells. *Biochem J.* 1993;289:71-79.
56. Low AM, Darby PJ, Kwan CY, Daniel EE. Effects of thapsigargin and ryanodine on vascular contractility: cross-talk between sarcoplasmic reticulum and plasmalemma. *Eur J Pharmacol.* 1993;230:53-62.
57. Chin TY, Lin HC, Kuo JP, Chueh SH. Dual effect of thapsigargin on cell death in porcine aortic smooth muscle cells. *Am J Physiol Cell Physiol.* 2007;292:383-395.
58. Humez S, Legrand G, Vanden-Abeele F, et al. Role of endoplasmic reticulum calcium content in prostate cancer cell growth regulation by IGF and TNFα. *J Cell Physiol.* 2004;201:201-213.
59. Goodman OB, Febbratio M, Simantov R, et al. Neprilysin inhibits angiogenesis via proteolysis of fibroblast growth factor-2. *J Biol Chem.* 2006;281:33597-33605.
60. Yang SP, Bae DG, Kang HJ, et al. Co-accumulation of vascular endothelial growth factor with β-amyloid in the brain of patients with Alzheimer's disease. *Neurobiol Aging.* 2004;25:283-290.
61. Cantara S, Donnini S, Morbidelli L, et al. Physiological levels of amyloid peptides stimulate the angiogenic response through FGF-2. *FASEB J.* 2004;15:1943-1945.
62. Mark RJ, Hensley K, Butterfield DA, Mattson MP. Amyloid beta-peptide impairs ion-motive ATPase activities: evidence for a role in loss of neuronal Ca^{2+} homeostasis and cell death. *J Neurosci.* 1995;15:6239-6249.
63. Mark RJ, Lovell MA, Markesbery WR, Uchida K, Mattson MP. A role for 4-hydroxynonenal, an aldehydic product of lipid peroxidation, in disruption of ion homeostasis and neuronal death induced by amyloid beta-peptide. *J Neurochem.* 1997;68:255-264.

Available online at www.sciencedirect.com
ScienceDirect
Neurochemistry International 52 (2008) 683–687
NEUROCHEMISTRY International
www.elsevier.com/locate/neuint

Presenilin-1 mutation activates the signaling pathway of caspase-4 in endoplasmic reticulum stress-induced apoptosis

Futoshi Yukioka [a,b,1], Shinsuke Matsuzaki [a,b,c,1,*], Keisuke Kawamoto [a,b], Yoshihisa Koyama [a,b], Junichi Hitomi [d], Taiichi Katayama [e], Masaya Tohyama [a,b,c]

[a] *Department of Anatomy and Neuroscience, Graduate School of Medicine, Osaka University, 2-2 Yamadaoka, Suita, Osaka 565-0871, Japan*
[b] *The 21st Century COE program, Japan*
[c] *The Osaka-Hamamatsu Joint Research Center For Child Mental Development, Japan*
[d] *Department of Cell Biology, Harvard Medical School, 240 Longwood Avenue, Boston, MA 02115, USA*
[e] *Department of Anatomy and Neuroscience, Hamamatsu University School of Medicine, 1-20-1 Handayama, Hamamatsu, Shizuoka 431-3192, Japan*

Received 3 July 2007; received in revised form 24 August 2007; accepted 30 August 2007
Available online 4 September 2007

Abstract

In the previous reports, we showed that the familial Alzheimer's disease (AD)-linked presenilin-1 (PS1) mutation induced the fragility to the endoplasmic reticulum (ER) stress and that caspase-4 mediates ER stress-induced- and β-amyloid induced-apoptotic signaling in human cells. These results suggest the involvement of ER stress and caspase-4 in the cell death observed in AD. In this report, we studied the activation of caspase-4 in the familial AD-linked PS1 mutation (ΔE9). Cleavage of caspase-4 under ER stress was enhanced by the overexpression of the familial AD-linked mutation (ΔE9), showing that caspase-4 is a key caspase involved in the apoptotic signaling of AD. We also showed that the overexpression of caspase-4 induced cleavage of caspase-9 and caspase-3 without releasing cytochrome-*c* from the mitochondria. Thus, caspase-4 activates downstream caspases independently of mitochondrial apoptotic signaling and this might contribute to the pathogenesis of AD.

To sum up our data, the familial AD-linked PS1 mutation accelerates the cleavage of caspase-4 under the ER stress and results in the activation of caspase-9 and caspase-3, apoptosis signal, without releasing cytochrome-*c*.

Keywords: Caspase-4; Caspase-3; Caspase-9; Familial AD-linked presenilin-1 mutation; ER stress; Mitochondria; Alzheimer's disease

1. Introduction

Missense mutations in the human presenilin-1 (PS1) gene, which are found on chromosome 14, cause early-onset familial Alzheimer's disease (AD) (Sherrington et al., 1995). We have shown that familial AD-linked PS1 mutations increase vulnerability to endoplasmic reticulum (ER) stress by altering the unfolded-protein response (UPR) (Katayama et al., 1999). Caspase-12 has been shown to be involved in signaling pathways specific to ER stress-induced apoptosis (Nakagawa et al., 2000; Yoneda et al., 2001). Pro-caspase-12, which is predominantly localized in the ER, is specifically cleaved by ER stress, and caspase-12-deficient mice show a reduced sensitivity to amyloid-β (Aβ) (Nakagawa et al., 2000), which induces neuronal cytotoxicity (Yankner et al., 1989). Thus, caspase-12 has been suggested to play a key role in the pathogenesis of AD. However, it has been controversial whether similar mechanisms are working in the human (Katayama et al., 1999; Rao et al., 2001; Fischer et al., 2002). In humans, although the caspase-12 gene is transcribed into mRNA, mature caspase-12 protein would not be produced because the gene is interrupted by a frame shift and a premature stop codon (Fischer et al., 2002). Thus, human caspase-12 does not function in ER stress-induced apoptosis such as in AD, although some other caspases with similar structures might substitute functionally for caspase-12 in the human. Recently,

* Corresponding author at: Department of Anatomy and Neuroscience, Graduate School of Medicine, Osaka University, 2-2 Yamadaoka, Suita, Osaka 565-0871, Japan. Tel.: +81 6 6879 3221; fax: +81 6 6879 3229.
E-mail address: s-matsuzaki@anat2.med.osaka-u.ac.jp (S. Matsuzaki).
[1] Contributed equally to this work.

0197-0186/$ – see front matter © 2007 Elsevier Ltd. All rights reserved.
doi:10.1016/j.neuint.2007.08.017

we have revealed that caspase-4 can function as an ER stress-induced caspase in humans and may be involved in pathogenesis of AD (Hitomi et al., 2004). However, little is known about the downstream actions of caspase-4, though caspase-3 and caspase-9 are suggested to exist downstream from caspase-12 (Morishima et al., 2002). In the present study, we found that the familial AD-linked PS1 mutation accelerates the cleavages of caspase-4 to induce neuronal death, showing that caspase-4 is involved in the pathogenesis of familial AD. We also showed that the activation of caspase-4 activates caspase-3 and caspase-9 without involving the cytochrome-*c* pathway.

2. Materials and methods

2.1. Chemicals and antibodies

We used the following antibodies: anti-caspase-4 mAb (4B9; MBL International Corporation, Nagoya, Japan), anti-caspase-3 mAb (Cell Signaling Technology, Beverly, MA), anti-cytochrome-*c* pAb (MBL International Corporation), anti-β-actin mAb (C4; CHEMICON International Inc., Temecula, CA), anti-caspase-9 mAb (5B4; MBL International Corporation), anti-PUMA pAb (Sigma–Aldrich, St. Louis, MO), HRP-conjugated anti-mouse IgG antibody (Cell Signaling Technology) and HRP-conjugated anti-rabbit IgG antibody (Cell Signaling Technology). All antibodies were diluted to PBS containing 0.05% Tween-20. The chemical reagents used in this experiment were tunicamycin, thapsigargin and staurosporine (Sigma–Aldrich).

2.2. Cell culture

SK-N-SH cells and COS-7 cells were cultured in α-MEM (Invitrogen, Carlsbad, CA) and DMEM (Invitrogen), respectively, both containing 10% FBS, at 37 °C under 5% CO_2. SK-N-SH neuroblastoma cell lines stably expressing wild-type PS1 or PS1ΔE9 have been described previously (Katayama et al., 1999).

2.3. cDNA cloning

The expression plasmids for caspase-4 tagged the FLAG sequence at the 3′ end (the resultant constructs were termed caspase-4-FLAG) and FLAG have been described previously (Hitomi et al., 2004). We constructed the pcDNA3.1 (+) expression vector (Invitrogen) carrying the full-length human *caspase-4* cDNA encoding 854 (NM_001225) amino acids fused in-frame with the GFP sequence at the 3′ end and GFP (the resultant constructs were termed caspase-4-GFP and GFP, respectively).

2.4. Subcellular fractionation

COS-7 cells cultured on a 10-cm dish were washed twice with PBS, harvested and suspended in buffer A (50 mM Tris–HCl, pH 8.0, 1 mM EDTA, 0.32 M sucrose, 0.1 mM PMSF) for 5 min on ice. Then the cells were passed through a 25-gauge needle 13 times and centrifuged at 500 × *g* for 10 min to collect a crude nuclear pellet. The supernatant was centrifuged at 1200 × *g* for 10 min to yield a mitochondria-enriched pellet and this supernatant was collected as a cytosolic fraction. The mitochondria-enriched pellets were dissolved in buffer A containing 0.3% triton. An equal volume of each fraction was subjected to Western blotting as described below, using the indicated antibodies.

2.5. Western blot analysis

Cells treated with the indicated reagents were washed twice with PBS, harvested, and lysed in TNE buffer (10 mM Tris–HCl, pH 7.8, 1 mM EDTA, 150 mM NaCl, 1 mM PMSF) containing 0.5% NP-40 and protease inhibitor cocktail (Roche, Sydney, Australia). Equal amounts of protein were subjected to 12% SDS-PAGE for caspase-4, caspase-9 and caspase-3 or 15% SDS-PAGE for cytochrome-*c* and transferred to a PVDF membrane (Millipore, Bedford, MA). The membrane was blocked with 5% skim milk and incubated with each primary antibody (anti-caspase-4 mAb, 1:1000; anti-caspase-9 mAb, 1:1000; anti-caspase-3 mAb, 1:1000; anti-cytochrome-*c* pAb, 1:200; anti-β-actin mAb, 1:2000; anti-PUMA pAb 1:1000) followed by incubation with an HRP-conjugated secondary antibody (anti-mouse IgG antibody, 1:1000; anti-rabbit IgG antibody, 1:1000). Proteins were visualized with an ECL detection system (Amersham Biosciences, Piscataway, NJ).

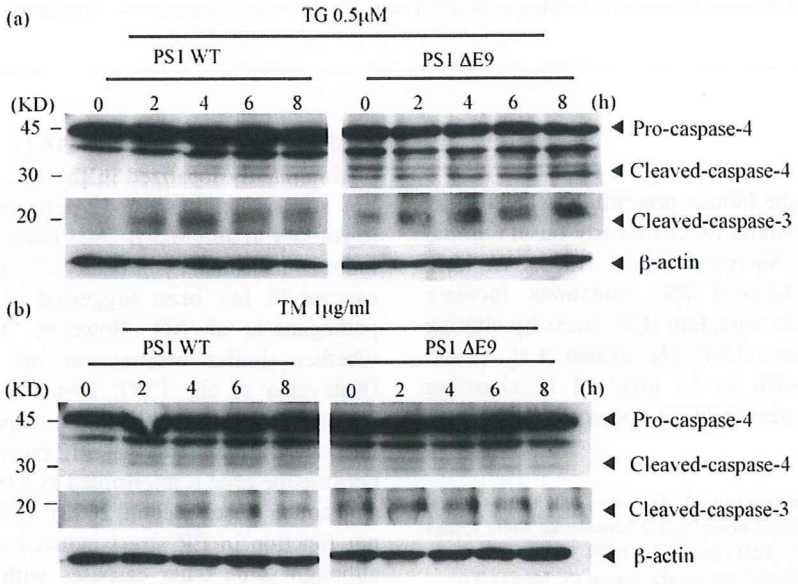

Fig. 1. FAD-linked mutation accelerates the cleavage of caspase-4 and caspase-3 under ER stress. SK-N-SH cells stably expressing PS1 (PS1WT) (a and b left panels) and mutant PS1 lacking exon 9 (PS1ΔE9) (a and b right panels) were treated with 0.5 μM thapsigargin (TG) (a) or 1 μg/ml tunicamycin (TM) (b) followed by incubation for indicated periods. Equal amounts of cell lysates were analyzed by Western blotting using anti-caspase-4 (upper panels of a and b), anti-caspase-3 (middle panels of a and b) or anti-β-actin (lower panels of a and b) antibody.

3. Results

3.1. PS1 mutation accelerated the cleavage of caspase-4 under ER stress

Familial AD-linked PS1 mutations, such as a deletion of exon 9 (PS1ΔE9), increase the vulnerability to ER stress by altering the UPR. ER stresses induce increased cell death in cells expressing mutant PS1 as compared with cells expressing the wild-type PS1. Caspase-4 and caspase-12 localized to the ER membrane are involved in the pathogenesis of neuronal death caused by ER stress in humans and rodents, respectively (Hitomi et al., 2004; Nakagawa et al., 2000). To determine the effect of PS1 mutation on the cleavage of caspases under ER stress, we studied the level of the cleavage of caspase-4 and caspase-3 after treatment with thapsigargin, an ER Ca-ATPase inhibitor, using wild-type PS1 or PS1ΔE9 expressing cells. Before thapsigargin treatment, we pretreated the cells with fresh medium for more than 1 h to obtain baseline data. After pre-incubation, the cells were exposed to 0.5 μM thapsigargin or 1 μg/ml tunicamycin. In wild-type PS1 cells, the cleaved form of caspase-4 and caspase-3 could not be identified under the basal condition and increased gradually after the addition of thapsigargin (Fig. 1a). In PS1ΔE9 cells, the cleaved forms of caspase-4 and caspase-3 were detected in the basal condition (Fig. 1a). The activation pattern of caspase-4 and caspase-3 under ER stress was correlated with each other, suggesting a close functional association between caspase-4 and caspase-3. The acceleration of the cleavage of caspase-4 and caspase-3 in PS1ΔE9 expressing cells were also induced by tunicamycin (Fig. 1b).

3.2. Caspase-4 induced the cleavage of caspase-9 and caspase-3

Next, we examined whether activation of caspase-4 induces the cleavage of caspase-3 or caspase-9. Caspase-4-FLAG or FLAG was overexpressed in COS-7 cells and there were effects of caspase-4 on the cleavage of caspase-3 and caspase-9. As a positive control of cleaved caspase-9 or caspase-3, the lysates of 0.1 μM staurosporin-treated COS-7 cells were used (Fig. 2b and c). Overexpression of caspase-4-FLAG, which caused the cleavage of caspase-4 in a self-(auto-)cleavage manner 24 h after overexpression of caspase-4-FLAG (Fig. 2a), induced remarkable cleavage of endogenous caspase-9 (Fig. 2b) and endogenous caspase-3 (Fig. 2c) in a concentration-dependent manner and such effects could not be detected in the control vector expressing cells (Fig. 2b and c). These results suggest that caspase-3 and capase-9 exist downstream from caspase-4.

3.3. Overexpression of caspase-4 did not affect on the efflux of cytochrome-c

Long exposure to ER stress influences mitochondrial function *via* PUMA (the Bcl-2 homology domain 3-only family member) (Reimertz et al., 2003) and mitochondrial dysfunction causes the activation of caspase-9 and caspase-3.

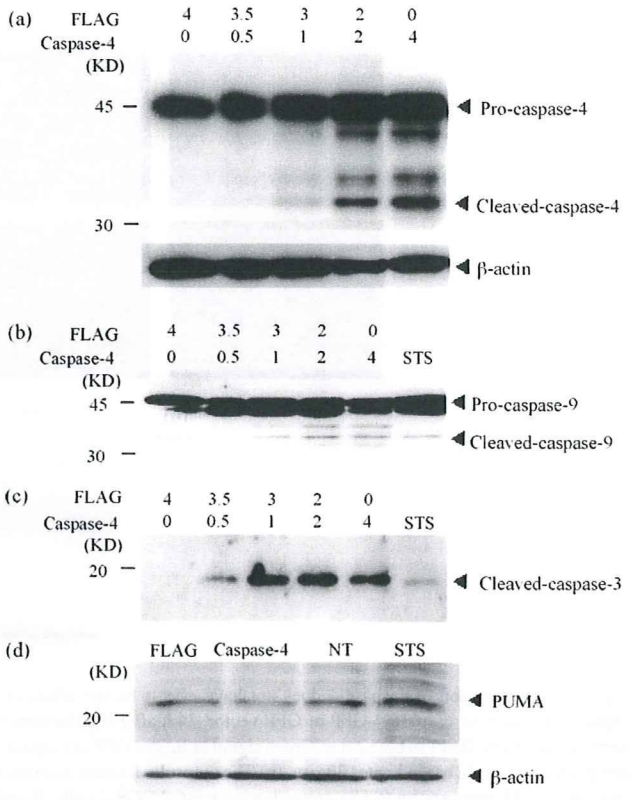

Fig. 2. Overexpression of caspase-4 increases the cleavage of caspase-3 and caspase-9. (a–c) COS-7 cells were transfected with the mixture of expression vectors for caspase-4-FLAG and FLAG as shown in this figure (0, 0.5, 1, 2 or 4 μg of caspase-4-FLAG expression vector were mixed with FLAG expression vector and total volume of each mixtures of the expression vectors was 4 μg). Twenty-four hours after transfection, equal amounts of cell lysates were analyzed by Western blotting using anti-caspase-4 (a), anti-caspase-9 (b) or anti-caspase-3 (c) antibody. As a positive control of cleaved caspase-9 or caspase-3, the lysates of 0.1 μM staurosporin (STS) -treated COS-7 cells were used. (d) Lysates of COS-7 cells transfected with 2 μg of expression vector for caspase-4-FLAG or FLAG were analyzed by Western blotting using anti-PUMA antibody. Overexpression of caspase-4 failed in the induction of PUMA, while STS treatment increased the expression level of PUMA in comparison with no treated COS-7 cells (NT) used as a negative control.

Thus, we examined the possibility that cleavage of caspase-9 and caspase-3 induced by the overexpression of caspase-4 is attributable to the mitochondrial dysfunction *via* activation of PUMA, but caspase-4 did not induce PUMA (Fig. 2d). These findings suggest that activation of caspase-3 and caspase-9 does not depend on the activation of PUMA, which causes the mitochondrial dysfunction. Next, we investigated whether caspase-4 provokes the effluent of cytochrome-*c* from mitochondria to cytosol using immunocytochemistry and Western blotting of subcellular fractionation. Either caspase-4-GFP or GFP, as a control, was overexpressed in COS-7 cells. The punctate distribution pattern of cytochrome-*c* observed in the cytoplasm of either caspase-4-GFP or GFP expressing COS-7 cells was similar to that of the no treatment cells (Fig. 3a). On the other hand, STS-treated cells showed a diffused distribution of cytochrome-*c* in cytoplasm (Fig. 3a). These results suggest that caspase-4 does not cause the release of cytochrome-*c*. To confirm this, we collected the cytosolic

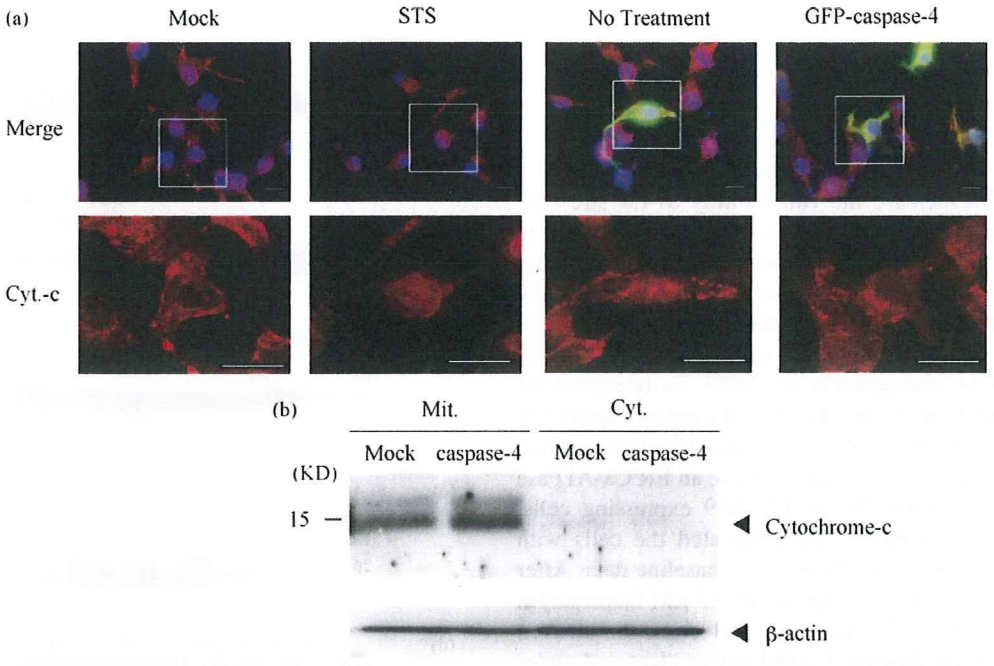

Fig. 3. Overexpression of caspase-4 does not have effects on the efflux of cytochrome-*c* from mitochondria to cytosol. (a) COS-7 cells were transfected with expression vector for caspase-4-GFP or GFP vector. 24 h after transfection, the cell were fixed and immunostained with anti-cytochrome-*c* antibody (red). Nuclei were visualized by DAPI as blue color. Green signal indicates GFP or caspase-4-GFP expressing cells. Lower panels show enlarged pictures of inserted boxes in each merged figures. Scale bar indicates 20 μm. (b) The cytosolic fraction and mitchondrial fraction were collected from the FLAG or caspase-4-FLAG expressing COS-7 cells or 0.1 μM staurosporin (STS) -treated or no treated COS-7 cells. Equal amounts of cell lysates were analyzed by Western blotting using anti-cytochrome-*c* (upper panel: the bands around 15 kDa indicate cytochrome-*c*) or anti- β-actin (lower panel) antibody.

fraction and mitchondrial fraction from the cells expressing caspase-4-FLAG or FLAG. Cytochrome-*c* could not be detected from the cytosol fraction of these cells (Fig. 3b). These data, with the previously described data, suggest that caspase-4 could activate caspase-9 and caspase-3 independently of the mitchondria-cytchrome-c pathway.

4. Discussion

Since caspase-12 has been shown to be involved in signaling pathways specific to ER stress-induced apoptosis (Nakagawa et al., 2000), caspase-12 has been believed to be involved in the pathogenesis of AD. However, since mature caspase-12 protein is not produced in humans (Fischer et al., 2002), caspase-12 does not function in ER stress-induced apoptosis such as AD, and some other caspases may play a key role in humans. Recently, we have found that caspase-4 can function as an ER stress-induced caspase in humans and may be involved in the pathogenesis of AD (Hitomi et al., 2004). The present study revealed that the familial AD-linked mutation (PS1ΔE9) enhances the cleavage of caspase-4 (Fig. 1) suggesting that caspase-4 plays a key role in the pathogenesis of AD.

Caspase-12-deficient mice show a reduced susceptibility to Aβ toxicity (Nakagawa et al., 2000). In humans, in which caspase-12 protein is not produced, caspase-4 functions similarly to mouse caspase-12 and is cleaved specifically by ER stress and Aβ treatment (Hitomi et al., 2004). Cell death induced by Aβ treatment is also partially inhibited by RNAi to caspase-4 (Hitomi et al., 2004). Thus, it is probable that in the human brain caspase-4 is involved in Aβ-induced cell death. From the aspect of Aβ, it could be concluded that activation of caspase-4 by ER stress and familial AD-linked mutations elevate the vulnerability of neurons to apoptosis, and is involved in the pathogenesis of AD.

Downstream events from caspase-4 are not fully understood. The present study has revealed that overexpression of caspase-4 results in the cleavage of caspase-3 and caspase-9 without the release of cytochrome-*c* from the mitochondria (Figs. 2 and 3). These findings indicate that caspase-4 functions using similar signaling pathways to caspase-12, which has been reported to activate downstream caspase-9 independently of cytochrome-*c* release (Morishima et al., 2002). But a clear mechanism of cleavage of caspase-3 and caspase-9 by ER stress is still obscure. PUMA, one of the BH3-only proteins, is induced *via* the p53 cascade under long term ER stress (Reimertz et al., 2003; Li et al., 2006). Induction of PUMA causes the dysfunction of mitochondria and the efflux of cytochrome-*c* from mitochondria to the cytosol, resulting in cell death through the activation of caspase-3 (Li et al., 2006). Accordingly, activation of caspase-3 and caspase-9 by the ER stress-induced cleavage of caspase-4 might be attributable to PUMA. However, in the present study, the overexpression of caspase-4 failed to induce the expression of PUMA, suggesting a lesser involvement of PUMA in the activation of caspase-3 and caspase-9 *via* caspase-4 (Fig. 2d). A faint relationship between mitochondrial function and capase-4 was also demonstrated by our previous study (Hitomi et al., 2004). Cleavage of caspase-4 is not affected by the overexpression of

Bcl-2, which prevents signal transduction on the mitochondria. In addition, the overexpression of caspase-4 failed to induce the efflux of cytochrome-*c* from mitochondria to cytosol (Fig. 3). Thus, caspase-4 could directly cleave caspase-3 and caspase-9 and induce cell death without involvement of mitochondrial apoptotic machinery.

In addition to AD, we have established that neuronal death caused by ischemia is also attributable to ER stress (Bando et al., 2003). Recently, the involvement of ER stress in neuronal death in Huntington's disease (Kouroku et al., 2002), Parkinson's disease (Ryu et al., 2002) and amyotrophic lateral sclerosis (Atkin et al., 2006) has been reported. Based upon these findings, it is likely that the activation of caspase-4 mediates neuronal cell death, not only in the AD, but also other neurodegenerative disorders. Accordingly, caspase-4 could be a potential target for the development of treatments for neurodegenerative diseases. For this purpose, it is important to screen the proteins interacting with pro-caspase-4.

Acknowledgements

This work was supported by grants from the Osaka Medical Research Foundation For Incurable Diseases. We are grateful Ms. Arakawa, Ms. Moriya and Ms. Ohashi for preparing the experiments.

References

Atkin, J.D., Farg, M.A., Turner, B.J., Tomas, D., Lysaght, J.A., Nunan, J., Rembach, A., Nagley, P., Beart, P.M., Cheema, S.S., Horne, M.K., 2006. Induction of the unfolded protein response in familial amyotrophic lateral sclerosis and association of protein-disulfide isomerase with superoxide dismutase 1. J. Biol. Chem. 281, 30152–30165.

Bando, Y., Katayama, T., Kasai, K., Taniguchi, M., Tamatani, M., Tohyama, M., 2003. GRP94 (94 kDa glucose-regulated protein) suppresses ischemic neuronal cell death against ischemia/reperfusion injury. Eur. J. Neurosci. 18, 829–840.

Fischer, H., Koenig, U., Eckhart, L., Tschachler, E., 2002. Human caspase 12 has acquired deleterious mutations. Biochem. Biophys. Res. Commun. 293, 722–726.

Hitomi, J., Katayama, T., Eguchi, Y., Kudo, T., Taniguchi, M., Koyama, Y., Manabe, T., Yamagishi, S., Bando, Y., Imaizumi, K., Tsujimoto, Y., Tohyama, M., 2004. Involvement of caspase-4 in endoplasmic reticulum stress-induced apoptosis and Abeta-induced cell death. J. Cell Biol. 165, 347–356.

Katayama, T., Imaizumi, K., Sato, N., Miyoshi, K., Kudo, T., Hitomi, J., Morihara, T., Yoneda, T., Gomi, F., Mori, Y., Nakano, Y., Takeda, J., Tsuda, T., Itoyama, Y., Murayama, O., Takashima, A., St. George-Hyslop, P., Takeda, M., Tohyama, M., 1999. Presenilin-1 mutations downregulate the signalling pathway of the unfolded-protein response. Nat. Cell Biol. 1, 479–485.

Kouroku, Y., Fujita, E., Jimbo, A., Kikuchi, T., Yamagata, T., Momoi, M.Y., Kominami, E., Kuida, K., Sakamaki, K., Yonehara, S., Momoi, T., 2002. Polyglutamine aggregates stimulate ER stress signals and caspase-12 activation. Hum. Mol. Genet. 11, 1505–1515.

Li, J., Lee, B., Lee, A.S., 2006. Endoplasmic reticulum stress-induced apoptosis: multiple pathways and activation of p53-up-regulated modulator of apoptosis (PUMA) and NOXA by p53. J. Biol. Chem. 281, 7260–7270.

Morishima, N., Nakanishi, K., Takenouchi, H., Shibata, T., Yasuhiko, Y., 2002. An endoplasmic reticulum stress-specific caspase cascade in apoptosis. Cytochrome c-independent activation of caspase-9 by caspase-12. J. Biol. Chem. 277, 34287–34294.

Nakagawa, T., Zhu, H., Morishima, N., Li, E., Xu, J., Yankner, B.A., Yuan, J., 2000. Caspase-12mediates endoplasmic-reticulum-specific apoptosis and cytotoxicity by amyloid-beta. Nature 403, 98–103.

Rao, R.V., Hermel, E., Castro-Obregon, S., del Rio, G., Ellerby, L.M., Ellerby, H.M., Bredesen, D.E., 2001. Coupling endoplasmic reticulum stress to the cell death program. Mechanism of caspase activation. J. Biol. Chem. 276, 33869–33874.

Reimertz, C., Kogel, D., Rami, A., Chittenden, T., Prehn, J.H., 2003. Gene expression during ER stress-induced apoptosis in neurons: induction of the BH3-only protein Bbc3/PUMA and activation of the mitochondrial apoptosis pathway. J. Biol. Chem. 162, 587–597.

Ryu, E.J., Harding, H.P., Angelastro, J.M., Vitolo, O.V., Ron, D., Greene, L.A., 2002. Endoplasmic reticulum stress and the unfolded protein response in cellular models of Parkinson's disease. J. Neurosci. 22, 10690–10698.

Sherrington, R., Rogaev, E.I., Liang, Y., Rogaeva, E.A., Levesque, G., Ikeda, M., Chi, H., Lin, C., Li, G., Holman, K., Tsuda, T., Mar, L., Foncin, J.F., Bruni, A.C., Montesi, M.P., Sorbi, S., Rainero, I., Pinessi, L., Nee, L., Chumakov, I., Pollen, D., Brookes, A., Sanseau, P., Polinsky, R.J., Wasco, W., Da Silva, H.A.R., Haines, J.L., Pericak-Vance, M.A., Tanzi, R.E., Roses, A.D., Fraser, P.E., Rommens, J.M., St. George-Hyslop, P., 1995. Cloning of a gene bearing missense mutations in early-onset familial Alzheimer's disease. Nature 375, 754–760.

Yankner, B.A., Dawes, L.R., Fisher, S., Villa-Komaroff, L., Oster-Granite, M.L., Neve, R.L., 1989. Neurotoxicity of a fragment of the amyloid precursor associated with Alzheimer's disease. Science 245, 417–420.

Yoneda, T., Imaizumi, K., Oono, K., Yui, D., Gomi, F., Katayama, T., Tohyama, M., 2001. Activation of caspase-12, an endoplastic reticulum (ER) resident caspase, through tumor necrosis factor receptor-associated factor 2-dependent mechanism in response to the ER stress. J. Biol. Chem. 276, 13935–13940.

Gene and Expression Analyses Reveal Enhanced Expression of Pericentrin 2 (*PCNT2*) in Bipolar Disorder

Ayyappan Anitha, Kazuhiko Nakamura, Kazuo Yamada, Yoshimi Iwayama, Tomoko Toyota, Nori Takei, Yasuhide Iwata, Katsuaki Suzuki, Yoshimoto Sekine, Hideo Matsuzaki, Masayoshi Kawai, Ko Miyoshi, Taiichi Katayama, Shinsuke Matsuzaki, Kousuke Baba, Akiko Honda, Tsuyoshi Hattori, Shoko Shimizu, Natsuko Kumamoto, Masaya Tohyama, Takeo Yoshikawa, and Norio Mori

Background: DISC1 has been suggested as a causative gene for psychoses in a large Scottish kindred. PCNT2 has recently been identified as an interacting partner of DISC1. In this study, we investigated the role of PCNT2 in bipolar disorder, by gene expression analysis and genetic association study.

Methods: By TaqMan real-time quantitative reverse transcriptase polymerase chain reaction (qRT-PCR), we examined the messenger RNA (mRNA) levels of PCNT2 in the postmortem prefrontal cortex of bipolar disorder ($n = 34$), schizophrenia ($n = 31$), and control subjects ($n = 32$), obtained from Stanley Array Collection. We also compared the mRNA levels of PCNT2 in the peripheral blood lymphocytes of bipolar disorder ($n = 21$), schizophrenia ($n = 21$), depression ($n = 33$), and control subjects ($n = 57$). For the association study, 23 single nucleotide polymorphisms (SNPs) were analyzed in 285 bipolar disorder patients and 287 age-and gender-matched control subjects, all of Japanese origin. The genotypes were determined by TaqMan assay.

Results: Significantly higher expression of PCNT2 was observed in the brain samples of bipolar group, compared with the control ($p = .001$) and schizophrenia ($p = .018$) groups. In the peripheral blood lymphocytes also, a significantly higher expression of PCNT2 was observed in the bipolar group, compared with the control subjects ($p = .043$). However, none of the SNPs analyzed in our study showed a significant association with bipolar disorder; a weak tendency toward association was observed for two intronic SNPs.

Conclusions: Our findings suggest that elevated levels of PCNT2 might be implicated in the pathophysiology of bipolar disorder.

Key Words: Association study, bipolar disorder, DISC1, PCNT2, peripheral blood lymphocytes, postmortem prefrontal cortex

Bipolar disorder, which is the sixth highest cause of global disability (1), affects approximately 1% of the population worldwide (2). The molecular pathophysiology of the illness has been controversial, although the contribution of genetic factors has been evidenced by family, twin, and adoption studies (3).

Disrupted-in-schizophrenia 1 (*DISC1*) has been identified as a disrupted gene by a balanced translocation (1; 11)(q42.1; q14.3) that co-segregated with major psychiatric disorders in a large Scottish kindred (4–7); the translocation carriers in the family manifested a wide spectrum of psychiatric phenotypes including schizophrenia, bipolar disorder, and recurrent major depression (4). A subsequent independent study by Devon *et al.* (8) of a Scottish family affected with schizophrenia and bipolar disorder failed to detect either co-segregation with the disease status or significant association involving any of the markers of the *DISC1* gene. Nevertheless, recent studies report the association of *DISC1* polymorphisms with schizophrenia (9–12) and with bipolar disorder (13,14). Hence, *DISC1* might be involved in the pathophysiology of only a limited subset of major psychiatric disorders.

Recently, it has been proved that DISC1 is a multifunctional protein interacting with several cytoskeletal and centrosomal proteins via distinct domains (15–19). Thus, a signaling pathway involving DISC1 and its interacting proteins rather than the DISC1 molecule per se might be involved in the pathology of major psychiatric disorders.

The fasciculation and elongation protein-zeta 1 (FEZ1) (18) and kendrin or pericentrin 2 (PCNT2) (20) have recently been identified as interacting partners of DISC1. DISC1 has been shown to participate in neurite outgrowth through its interaction with FEZ1 (18); the PCNT2-binding region of DISC1 overlaps with the region interacting with FEZ1 (20). A study by Yamada *et al.* (21) had suggested that *FEZ1* might be associated with schizophrenia in Japanese cohorts.

The *PCNT2* gene is located on 21q22.3, which has been identified as a bipolar disorder susceptibility region (22). In this study, we compared the messenger RNA (mRNA) expression levels of *PCNT2* in samples from the postmortem prefrontal cortex of bipolar disorder patients and schizophrenia patients, obtained from the Stanley Array Collection. Because lymphocytes are now considered to be a convenient and accessible alternative to brain samples for biochemical and genetic investigations of the functions of the central nervous system (CNS) (23), we further compared the mRNA levels of *PCNT2* in the periph-

From the Department of Psychiatry and Neurology (AA, KN, NT, YaI, KS, YS, MK, NM), Hamamatsu University School of Medicine; Department of Anatomy and Neuroscience (TK), Hamamatsu University School of Medicine, Hamamatsu; Laboratory of Molecular Psychiatry (KY, YoI, TT, TY), RIKEN Brain Science Institute, Saitama; The Osaka-Hamamatsu Joint Research (HM, SM, MT), Center for Child Mental Development; Department of Anatomy and Neuroscience (SM, TH, SS, NK, MT), Graduate School of Medicine, Osaka University; The 21st Century COE program (SM, TH, SS, NK, MT); Pharmacology Research Laboratory (AH), Tanabe Seiyaku, Osaka; Department of Brain Science (KM), Graduate School of Medicine and Dentistry, Okayama University, Okayama; and the Department of Anatomy and Development Neurobiology (KB), School of Medicine, Kobe University, Kobe, Japan.

Address reprint requests to Kazuhiko Nakamura, M.D., Ph.D., Department of Psychiatry and Neurology, Hamamatsu University School of Medicine, Hamamatsu, 431-3192, Japan; E-mail: nakamura@hama-med.ac.jp.

Received April 17, 2007; revised July 13, 2007; accepted July 13, 2007.

0006-3223/08/$34.00
doi:10.1016/j.biopsych.2007.07.010

Table 1. Demographic Characteristics of the Control, Schizophrenia, and Bipolar Groups Examined in Brain mRNA Analysis

Variables	Control $n = 32$	Schizophrenia $n = 31$	Bipolar $n = 34$	p
Age (yrs) (mean ± SD)	44.2 ± 7.69	42.8 ± 7.83	45.3 ± 10.5	.51[a]
Male/Female	23/9	26/8	16/18	.02[b]
Race	32 White	30 White; 1 Hispanic	33 White; 1 Black	.646[c]
Postmortem Interval (hours)	29.9 ± 13.3	31.2 ± 16.5	37.0 ± 17.7	.16[a]
Brain pH	6.63 ± .25	6.47 ± .24	6.42 ± .30	.01[a]
Lifetime Dose of Antipsychotics[d]	—	89,360 ± 10,5400	10,040 ± 22,900	.0003[e]

mRNA, messenger RNA.
[a]One-way analysis of variance.
[b]χ^2 test.
[c]Fisher's Exact test.
[d]Fluphenazine equivalents.
[e]t test.

eral blood lymphocytes of bipolar disorder, schizophrenia, and depression cases. Because *PCNT2* expression was found to be enhanced in bipolar disorder, we also performed an association study of *PCNT2* in bipolar disorder.

Methods and Materials

Gene Expression Analysis

Brain RNA. The RNA from the dorsolateral prefrontal cortex (DLPFC; Brodmann's area 46) was donated by The Stanley Medical Research Institute (SMRI; http://www.stanleyresearch.org/programs/brain_collection.asp) (24). The RNA from 31 schizophrenia patients, 34 bipolar disorder patients, and 32 control subjects was used for the study; demographic details of the subjects are shown in Table 1. The schizophrenia patients were medicated; among the bipolar disorder group, 24 patients were medicated, and 10 were not medicated. All the schizophrenia patients exhibited psychotic features; in the bipolar disorder group, 21 patients showed psychotic features, and 11 were not psychotic. Because the RNA samples were coded, the diagnoses of the subjects were masked while the assays were performed. The study was approved by the Ethics Committee of Hamamatsu University School of Medicine.

Lymphocyte RNA. We obtained blood samples from 21 drug-naïve schizophrenia patients, 21 medicated bipolar disorder patients, and 57 healthy control subjects. Because all the bipolar disorder patients were inevitably medicated owing to the course of the disorder, we also included samples from 33 drug-naïve major depressive patients in this study.

All the control and patient samples were of Japanese origin. Patient groups were recruited from the Hamamatsu University Hospital, Japan, during the period from April 1, 2002 to September 30, 2003. The patients were diagnosed according to the DSM-IV (25), by senior psychiatrists (NK, IY, SK); the severity of symptoms was evaluated with the Brief Psychiatric Rating Scale (BPRS) (26) for patients with schizophrenia and with the Hamilton Depression Rating Scale (HAM-D) (27) for patients with depression. All the major depressive patients belonged to the single episode category (DSM-IV-Text Revision 296.2) (28). Among the 21 bipolar disorder patients, 14 were in remission states, 2 each were in hypomanic and manic states, and 3 in depressive state. Remission for bipolar disorder patients was defined as the absence of any apparent affective symptoms for a minimum of 6 months, without recurrence (25); this was verified via a direct interview with patients along with a review of clinical records.

Although patients with schizophrenia and those with depression had, by definition, never received medication, all the patients with bipolar disorder had been taking antipsychotic drugs; their lifetime doses of antipsychotic drugs were calculated in terms of chlorpromazine equivalents. Some of the patients had been taking antidepressant drugs and/or lithium also.

The healthy control subjects consisted of the staff at the hospital and volunteers from the community; they were recruited by poster advertisements and word of mouth in and around Hamamatsu city. Demographic details of the subjects who participated in the study are shown in Table 2. All of the subjects were presented with a complete description of the study, and their written informed consent was obtained for participation. The study was approved by the Ethics Committee of Hamamatsu University School of Medicine.

Peripheral blood (20 mL) was drawn from the cubital vein into ethylenediaminetetraacetic acid (EDTA)-containing plastic

Table 2. Demographic Characteristics of the Control, Schizophrenia, Bipolar and Depression Groups Examined in Lymphocyte mRNA Analysis

Variables	Control $n = 57$	Drug-Naïve Schizophrenia $n = 21$	Medicated Bipolar $n = 21$	Drug-Naïve Depression $n = 33$	p
Age (yrs) (mean ± SD)	29.8 ± 8.11	33.1 ± 11.7	47.3 ± 16.7	36.8 ± 13.2	<.001[a]
Male/Female	46/11	14/7	10/11	23/10	.04[b]
Lifetime Dose of Antipsychotics[c]	—	—	252 ± 539	—	
Lithium	—	—	760 ± 472	—	
Antidepressants	—	—	79.8 ± 114	—	

mRNA, messenger RNA.
[a]One-way analysis of variance.
[b]χ^2 test.
[c]Chlorpromazine equivalents.

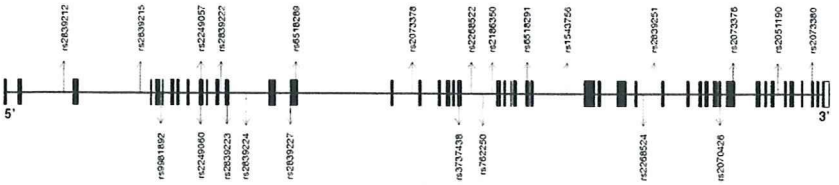

Figure 1. Genomic structure of *PCNT2*, and locations of single nucleotide polymorphisms (SNPs). Exons are indicated by boxes; SNP positions are denoted by arrows.

syringes. Lymphocytes were isolated from blood samples by the Ficoll-Paque gradient method; total RNA was extracted with RNAzolB reagent (Sawady, Tokyo, Japan), according to the manufacturer's instructions. We had been collecting blood samples at approximately the same time (10:00 AM) on the days assigned for sample collection; lymphocyte isolation and RNA extraction were done immediately thereafter. Thus, we maintained similar conditions during the collection and processing of all the samples. The RNA samples were quantified by analyzing the absorbance at 260 nm in a UV-spectrophotometer. Complementary DNA (cDNA) was synthesized by first strand reverse transcriptase reaction (RT) with Random Primer and M-MLV reverse transcriptase (Invitrogen, Carlsbad, California).

Quantitative Reverse Transcriptase Polymerase Chain Reaction. Real-time quantitative reverse transcriptase polymerase chain reaction (qRT-PCR) analysis was performed with the ABI PRISM 7900 Sequence Detection System (Applied Biosystems, Foster City, California). TaqMan primer/probes for *PCNT2* (NM_006031) and for glyceraldehyde-3-phosphate dehydrogenase (*GAPDH*; NM_002046), which served as the endogenous reference, were purchased from Applied Biosystems (Assay-on-Demand gene expression products Hs00195774 and Hs99999905, respectively). All reactions were performed in duplicate, according to the manufacturer's protocol. A comparative threshold cycle (C_T) method validation experiment was done to check whether the efficiencies of target and reference amplifications were approximately equal (the slope of the log input amount vs. $\Delta C_T < .1$). One sample was randomly chosen as the calibrator and was amplified in each plate, to correct for experimental differences among consecutive PCR runs. The amounts of *PCNT2* mRNA were normalized to the endogenous reference and expressed relative to the calibrator as $2^{-\Delta\Delta C_T}$ (comparative C_T method).

Statistical Analysis. Statistical calculations were performed with the SPSS statistical package, version 11.0.1 (SPSS, Tokyo, Japan). One-way analysis of variance (ANOVA) was used to examine the variability in the distribution of demographic variables across groups. Variability in *PCNT2* expression across the groups was analyzed with one-way ANOVA, followed by a post hoc analysis with the Tukey Honestly Significant Differences (HSD) test; to control for potential confounding factors, analysis of covariance (ANCOVA) was used. Any effect of various demographic variables upon *PCNT2* expression was examined by Pearson's correlation coefficient.

Association Study

Sample Information. We analyzed 285 bipolar disorder patients (age 48.0 ± 13.5 years [mean ± SD]; 157 male /128 female) and 287 age- and gender-matched healthy control subjects (age 48.0 ± 12.3 years, 146 male / 141 female). All the subjects were recruited from a geographical area located in the center of the mainland of Japan. Best-estimate lifetime diagnoses of patients were made by direct interview with two experienced psychiatrists, according to DSM-IV criteria (25), and with all available information from medical records, hospital staff, and family informants. Control subjects were recruited from hospital staff and company employees, documented to be free from any psychiatric problems, and were further interviewed by experienced psychiatrists to exclude any psychiatric disorders. This study was approved by the Ethics Committees of Hamamatsu University School of Medicine and RIKEN Brain Science Institute; written informed consent was obtained from all the participants.

Marker Selection. The genomic structure of *PCNT2* is based on the UCSC May 2004 draft assembly of the human genome (http://www.genome.ucsc.edu). The gene consists of 47 exons, spanning a genomic stretch of 121,587 bases (mRNA size 10,501 bases) (Figure 1). Single nucleotide polymorphisms (SNPs) for the association study were selected with the Applied Biosystems software SNPbrowser 3.5; we also referred to several databases for SNP information, including the National Centre for Biotechnology Information (NCBI dbSNP: http://www.ncbi.nlm.nih.gov/SNP) and Japanese Single Nucleotide Polymorphisms (JSNP: http://snp.ims.u-tokyo.ac.jp). On the basis of their genomic locations and minor allele frequencies (MAF > 0.1) in Japanese population, 23 SNPs were chosen for our analysis, to span the *PCNT2* gene as evenly as possible. We aimed at an average spacing of one common SNP at every 3–5 kb; however, this was not always possible, or practical. In some cases, there were long gaps with no validated common SNPs at the time we performed this study; furthermore, it was not possible to design suitable assays for some other SNPs. In addition to genotyping a common SNP at every possible 3–5 kb, we also checked the association of exonic SNPs within these intervals, to examine the possibility of *cis*-acting polymorphisms contributing to the altered expression of *PCNT2*.

Genotyping. Genomic DNA was extracted from whole blood with the QIAamp DNA blood kit (QIAGEN, Germantown, Maryland). The quality and quantity of DNA were estimated in a UV-Spectrophotometer.

Assay-on-Demand SNP genotyping products (Applied Biosystems) were used to score SNPs, on the basis of the TaqMan assay method (29). Genotypes were determined in the ABI 7900 Sequence Detection System (SDS) (Applied Biosystems) and analyzed with SDS v 2.0 software (Applied Biosystems).

Statistical Analysis. All the genotyping results were tested for Hardy-Weinberg Equilibrium (HWE). Any difference in allelic or genotypic distributions between patients and control subjects was evaluated with Fisher's exact test.

The haplotype frequencies of SNPs were estimated with the software COCAPHASE 2.403 (http://www.litbio.org/) (30). This software performs likelihood ratio tests under a logistic regression model of the probability that an allele or haplotype belongs to the case rather than the control group. The expectation maximization (EM) algorithm was used to resolve uncertain haplotypes, infer missing genotypes, and provide maximum-likelihood estimation of frequencies. Haplotype associations were also examined with this software.

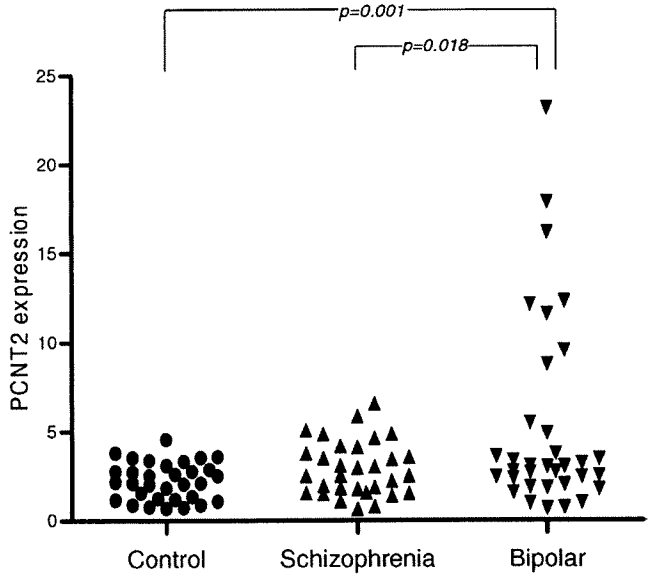

Figure 2. Post hoc pairwise comparison (Tukey Honestly Significant Differences) of *PCNT2* messenger RNA levels in the postmortem brains (Brodmann's area 46) from control, schizophrenia, and bipolar groups. A significant difference in *PCNT2* expression was observed between 1) control-bipolar (p = .001) and 2) schizophrenia-bipolar (p = .018) groups.

Results

Brain Samples

No significant difference in age [$F(2,97)$ = .69; p = .51], race distribution (Fisher's exact test p = .646), or postmortem intervals [$F(2,94)$ = 1.84; p = .16] was observed across the control, schizophrenia, and bipolar disorder groups. However, there was a significant group difference in gender distribution [$\chi^2(2)$ = 7.44; p = .02] and in brain pH [$F(2,94)$ = 5.23; p = .01] (Table 1). The control and schizophrenia groups had more men compared with the bipolar disorder group; brain pH was lower in the schizophrenia and bipolar disorder groups than that in the control group. In addition, the lifetime dose of antipsychotic drugs in the schizophrenia group was significantly higher than that in the bipolar disorder group [$t(32)$ = 4.10; p = .0003].

There was a significant difference in *PCNT2* expression across the three groups [$F(2,94)$ = 7.23; p = .001] (Figure 2). Subsequent post hoc pairwise comparison with Tukey HSD revealed a significantly higher expression of *PCNT2* in the bipolar disorder group (5.26 ± 5.47 [mean ± SD]), compared with the control (2.22 ± 1.06; p = .001) and schizophrenia (2.91 ± 1.53; p = .018) groups. The *PCNT2* expression did not differ between the control and schizophrenia groups (p = .70). After adjusting for gender and brain pH as potential confounders, with ANCOVA, the difference in *PCNT2* expression across the three groups remained significant [$F(2,92)$ = 3.77; p = .027]. The bipolar disorder group had a significantly higher expression of *PCNT2* in comparison with the control group (p = .045) but not in comparison with the schizophrenia group (p = .077). The difference in *PCNT2* expression between schizophrenia and bipolar disorder groups was significant (p = .017) when lifetime dose of antipsychotic drugs was considered as a confounding factor.

There was no significant difference [$t(30)$ = −1.114; p = .274] in *PCNT2* expression between the psychotic and non-psychotic groups of bipolar disorder patients. In addition, there was no significant difference in *PCNT2* expression [$t(32)$ = −1.71; p = .097] between the medicated and non-medicated groups of bipolar disorder patients. There were no significant correlations between *PCNT2* expression and age of onset or duration of illness, in patients with bipolar disorder.

Lymphocyte Samples

With regard to demographic characteristics, there was a significant difference in the distribution of age [$F(3,127)$ = 11.82; p < .001] and gender [$\chi^2(3)$ = 8.29; p = .04] across the control, drug-naïve-schizophrenia, medicated bipolar disorder, and drug-naïve depression groups (Table 2). The bipolar disorder group was comparatively older and had a higher proportion of women, when compared with the other three groups.

A significant difference in *PCNT2* expression was observed across the four groups [$F(3,128)$ = 6.46; p < .001] (Figure 3). Post hoc pairwise comparison with Tukey HSD showed a significantly higher expression of *PCNT2* in both the bipolar disorder group (1.14 ± .38; p = .043) and the depression group (1.22 ± .48; p = .001) than in the control group (.88 ± .32). However, *PCNT2* expression in the schizophrenia group (.93 ± .35) did not differ from and was, in effect, almost identical to that of the control group (p = .95). In addition, individuals with bipolar disorder in a remission state (1.11 ± .34) showed a significantly higher expression of *PCNT2*, compared with the control group (p = .022).

When age and gender were adjusted for as potential confounders, with ANCOVA, the difference in *PCNT2* expression across the four groups remained significant [$F(3,125)$ = 3.82; p = .003]; a significantly higher expression of *PCNT2* was observed in the bipolar disorder group (p = .010) and in the depression group (p < .001) than in the control group. Because the bipolar disorder group was, by definition, all medicated and received antipsychotic medication previously and/or at the time of the study, we examined the correlation between the lifetime dose of antipsychotic drugs and *PCNT2* expression in this group. There

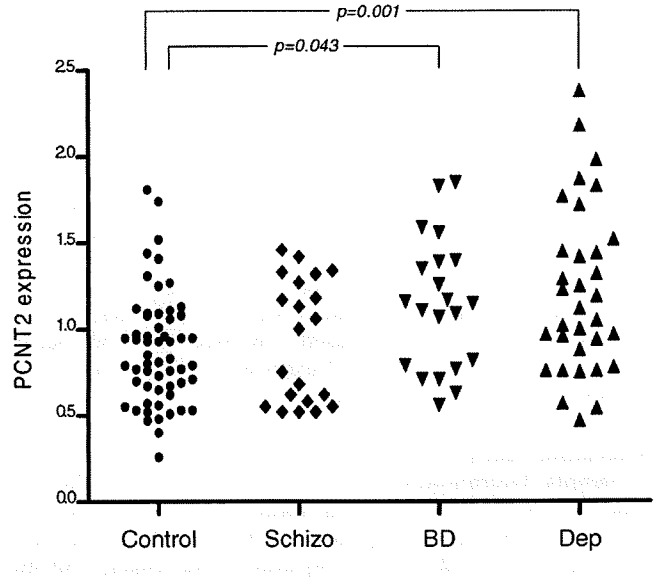

Figure 3. Post hoc pairwise comparison (Tukey Honestly Significant Differences) of *PCNT2* messenger RNA levels in the lymphocytes from control, drug-naïve schizophrenia (Schizo), medicated bipolar (BD), and drug-naïve depression (Dep) groups. A significant difference in *PCNT2* expression was observed between 1) control-bipolar (p = .043) and 2) control-dep (p = .001) groups.

Table 3. Allelic and Genotypic Distributions of PCNT2 SNPs

Marker	dbSNP ID	Samples	Allele (%)		*p*	Genotype (%)			*p*
SNP1	rs2839212		C	T		C/C	C/T	T/T	
	Intron 2	BP	428 (75.89)	136 (24.11)	.833	165 (58.51)	98 (34.75)	19 (6.74)	.515
		CT	431 (75.35)	141 (24.65)		160 (55.94)	111 (38.81)	15 (5.24)	
SNP2	rs2839215		G	A		G/G	G/A	A/A	
	Intron 3	BP	425 (75.62)	137 (24.38)	.756	163 (58.01)	99 (35.23)	19 (6.76)	.706
		CT	428 (74.83)	144 (25.17)		159 (55.59)	110 (38.46)	17 (5.94)	
SNP3	rs9981892		G	A		G/G	G/A	A/A	
	Intron 5	BP	423 (75.00)	141 (25.00)	.491	162 (57.45)	99 (35.11)	21 (7.45)	.56
		CT	439 (76.75)	133 (23.25)		168 (58.74)	103 (36.01)	15 (5.24)	
SNP4	rs2249057		C	A		C/C	C/A	A/A	
	Exon 10	BP	320 (56.74)	244 (43.26)	.985	90 (31.91)	140 (49.65)	52 (18.44)	.932
	(Silent)	CT	326 (56.79)	248 (43.21)		94 (32.75)	138 (48.08)	55 (19.16)	
SNP5	rs2249060		C	T		C/C	C/T	T/T	
	Exon 10	BP	428 (75.89)	136 (24.11)	.386	163 (57.80)	102 (36.17)	17 (6.03)	.472
	(Missense)	CT	448 (78.05)	126 (21.95)		172 (59.93)	104 (36.24)	11 (3.83)	
SNP6	rs2839222		A	G		A/A	A/G	G/G	
	Intron 12	BP	424 (75.44)	138 (24.56)	.349	163 (58.01)	98 (34.88)	20 (7.12)	.321
		CT	445 (77.80)	127 (22.20)		171 (59.79)	103 (36.01)	12 (4.20)	
SNP7	rs2839223		A	G		A/A	A/G	G/G	
	Exon 13	BP	430 (75.97)	136 (24.03)	.446	165 (58.30)	100 (35.34)	18 (6.36)	.506
	(Missense)	CT	447 (77.87)	127 (22.13)		172 (59.93)	103 (35.89)	12 (4.18)	
SNP8	rs2839224		G	A		G/G	G/A	A/A	
	Intron 13	BP	427 (75.98)	135 (24.02)	.468	165 (58.72)	97 (34.52)	19 (6.76)	.402
		CT	445 (77.80)	127 (22.20)		171 (59.79)	103 (36.01)	12 (4.20)	
SNP9	rs2839227		A	G		A/A	A/G	G/G	
	Exon 15	BP	428 (75.62)	138 (24.38)	.582	164 (57.95)	100 (35.34)	19 (6.71)	.640
	(Missense)	CT	442 (77.00)	132 (23.00)		169 (58.89)	104 (36.49)	14 (4.88)	
SNP10	rs6518289		C	T		C/C	C/T	T/T	
	Exon 15	BP	425 (75.62)	137 (24.38)	.534	164 (58.36)	97 (34.52)	20 (7.12)	.421
	(Missense)	CT	440 (77.19)	130 (22.81)		168 (58.95)	104 (36.49)	13 (4.56)	
SNP11	rs2073378		C	G		C/C	C/G	G/G	
	Intron 16	BP	428 (76.43)	132 (23.57)	.983	165 (58.93)	98 (35.00)	17 (6.07)	.74
		CT	439 (76.48)	135 (23.52)		166 (57.84)	107 (37.28)	14 (4.88)	
SNP12	rs3737438		C	T		C/C	C/T	T/T	
	Exon 21	BP	295 (51.94)	273 (48.06)	.158	79 (27.82)	137 (48.24)	68 (23.94)	.307
	(Silent)	CT	322 (56.10)	252 (43.90)		89 (31.01)	144 (50.17)	54 (18.82)	
SNP13	rs2268522		G	A		G/G	G/A	A/A	
	Intron 21	BP	407 (72.16)	157 (27.84)	.12	149 (52.84)	109 (38.65)	24 (8.51)	.126
		CT	390 (67.94)	184 (32.06)		128 (44.60)	134 (46.96)	25 (8.71)	
SNP14	rs762250		G	C		G/G	G/C	C/C	
	Intron 21	BP	407 (72.16)	157 (27.84)	.12	149 (52.84)	109 (38.65)	24 (8.51)	.126
		CT	390 (67.94)	184 (32.06)		128 (44.60)	134 (46.69)	25 (8.71)	
SNP15	rs2186350		A	G		A/A	A/G	G/G	
	Intron 21	BP	409 (72.52)	155 (27.48)	.08	150 (53.19)	109 (38.65)	23 (8.16)	.119
		CT	389 (67.77)	185 (32.23)		128 (44.60)	133 (46.34)	26 (9.06)	
SNP16	rs6518291		A	G		A/A	A/G	G/G	
	Exon 26	BP	430 (76.79)	130 (23.21)	.958	167 (59.64)	96 (34.29)	17 (6.07)	.705
	(Missense)	CT	440 (76.66)	134 (23.34)		167 (58.19)	106 (36.93)	14 (4.88)	
SNP17	rs1543756		G	A		G/G	G/A	A/A	
	Intron 27	BP	435 (76.86)	131 (23.14)	.827	169 (59.72)	97 (34.28)	17 (6.01)	.637
		CT	438 (76.31)	136 (23.69)		165 (57.49)	108 (37.63)	14 (4.88)	
SNP18	rs2268524		C	T		C/C	C/T	T/T	
	Intron 31	BP	295 (52.30)	269 (47.70)	.144	81 (28.72)	133 (47.16)	68 (24.11)	.214
		CT	325 (56.62)	249 (43.38)		90 (31.36)	145 (50.52)	52 (18.12)	
SNP19	rs2839251		C	T		C/C	C/T	T/T	
	Intron 31	BP	432 (76.33)	134 (23.67)	.83	167 (59.01)	98 (34.63)	18 (6.36)	.507
		CT	435 (75.78)	139 (24.22)		162 (56.45)	111 (38.68)	14 (4.88)	
SNP20	rs2070426		C	G		C/C	C/G	G/G	
	Exon 37	BP	410 (72.70)	154 (27.30)	.104	150 (53.19)	110 (39.01)	22 (7.80)	.107
	(Missense)	CT	392 (68.29)	182 (31.71)		128 (44.60)	136 (47.39)	23 (8.01)	

Table 3. (continued)

Marker	dbSNP ID	Samples	Allele (%)		*p*	Genotype (%)			*p*
SNP21	rs2073376		G	A		G/G	G/A	A/A	
	Exon 38	BP	410 (72.44)	156 (27.56)	.125	150 (53.00)	110 (38.87)	23 (8.13)	.107
	(Missense)	CT	392 (68.29)	182 (31.71)		128 (44.60)	136 (47.39)	23 (8.01)	
SNP22	rs2051190		T	C		T/T	T/C	C/C	
	Intron 41	BP	413 (72.71)	155 (27.29)	.102	152 (53.52)	109 (38.38)	23 (8.10)	.081
		CT	392 (68.29)	182 (31.71)		128 (44.60)	136 (47.39)	23 (8.01)	
SNP23	rs2073380		A	C		A/A	A/C	C/C	
	Exon 45	BP	293 (51.77)	273 (48.23)	.142	79 (27.92)	135 (47.70)	69 (24.38)	.225
	(Missense)	CT	322 (56.10)	252 (43.90)		88 (30.66)	146 (50.87)	53 (18.47)	

SNP, single nucleotide polymorphism; BP, bipolar; CT, control.

was no significant correlation between the lifetime dose of antipsychotic drugs and *PCNT2* expression ($r = -.066$, $p = .784$). In addition, no significant correlation was found between lithium doses and *PCNT2* expression ($r = -.349$, $p = .132$) or between antidepressant doses and *PCNT2* expression ($r = .412$, $p = .071$).

In patients with bipolar disorder and depression, there were no significant correlations between *PCNT2* expression and 1) age of onset, 2) duration of illness, or 3) HAM-D scores.

Association Study

Genotypic distributions of all the SNPs were found to be in HWE for the bipolar disorder group and its control subjects.

The allelic and genotypic frequencies of the 23 SNPs of *PCNT2* in the bipolar disorder and control groups are summarized in Table 3. None of the SNPs showed any significant difference in allelic or genotypic frequencies between the bipolar disorder and control groups. Tendencies for allelic and genotypic associations were observed for rs2186350 (SNP15) ($p = .0802$) and for rs2051190 (SNP22) ($p = .0814$), respectively. However, taking into account the multiple testing involved, these values become irrelevant. Haplotype analysis also failed to show any significant association.

Discussion

In this study, we observed a significantly higher expression of *PCNT2* in the brain and peripheral blood lymphocytes of bipolar disorder patients, when compared with the control subjects. The enhanced expression of *PCNT2* remained significant even after adjusting for the effect of various confounding variables; in addition, no correlation was observed between any of the medication doses and *PCNT2* expression. The lymphocyte samples from remission bipolar disorder patients and drug-naïve depression patients also showed elevated *PCNT2* expression. To our knowledge, this is the first study that has investigated *PCNT2* expression in the brain and peripheral blood lymphocytes of bipolar disorder patients.

Our findings lead us to hypothesize that *PCNT2* overexpression in the brain might contribute to the pathophysiology of bipolar disorder or could be the downstream result of some other aspect of the illness. PCNT2 has been proved to be essential for microtubule organization during cell division. In association with protein kinase A-anchoring proteins (AKAPs) and γ-tubulin ring complex (γ-TuRC), PCNT2 acts as a structural and regulatory scaffold at the centrosome, for those proteins that regulate cell cycle events (31–37). PCNT2 overexpression has been found to induce G2/antephase arrest of the cell cycle, followed by apoptosis, in COS cells. It has been proposed that the loss of the PCNT2-mediated anchoring mechanism due to its overexpression might elicit a checkpoint response that prevents mitotic entry and triggers apoptotic cell death (38). The exact molecular pathway involved in this process has yet to be identified. It is possible that PCNT2 overexpression might lead to some kind of apoptotic process in the brain, leading to its dysfunction. There are several studies that implicate apoptotic processes in the brain of bipolar disorder patients. At the histopathological level, striking reductions in neuronal density have been observed in the anterior cingulate cortex (ACCx) of bipolar disorder brains compared with schizophrenic brains (39). In addition, DNA fragmentation, which is a hallmark of apoptosis, has also been found to be increased in the ACCx of bipolar disorder subjects compared with schizophrenic subjects (40). Decreased glial number and density as well as decreased neuronal density have been reported in several regions of the frontal lobes, especially in the ACCx, of bipolar disorder brains (41). The recent hypothesis is that apoptosis might play a role in bipolar disorder and schizophrenia; however, considering the DNA damage, apoptosis is more likely to result in cell death in bipolar disorder patients but not in those with schizophrenia, in whom a more subtle perturbation in intracellular signaling might contribute to neuronal dysfunction (42). Abnormalities of PCNT2 can lead to defects in microtubule function, resulting in alterations in neuronal migration, axonal extension, and neurite outgrowth, thus leading to impaired neurodevelopment. Morphometric studies suggest that the pathophysiology of bipolar disorder includes anatomic abnormalities in the neural circuits interconnecting the prefrontal cortex, medial temporal lobe, and basal ganglia (43–45). In addition, recent studies provide evidence for a neurodevelopmental model of bipolar disorder, even though the effect might not be as pronounced as in the case of schizophrenia (46–52).

In this study, we found that the *PCNT2* expressions in peripheral blood lymphocytes were significantly higher in bipolar disorder and depressive patients than in control subjects. Lymphocytes are now considered to be a convenient and accessible alternative to brain samples for biochemical and genetic investigations of the functions of CNS, owing to the expression of neuroactive proteins and processes in lymphocytes and to altered lymphocyte functions in neuropsychiatric disorders; in addition, there are similarities of hormonal effects on the nervous system processes and lymphocyte physiology (23). Thus, the activity of the circulating blood leucocytes might be suggested to reflect the brain function. The expression of *PCNT2* in the peripheral blood lymphocytes might, therefore, be a useful biological marker of mood disorders.

The SMRI Online Genomics Database (http://www.stanleyresearch.org/brain/) reports reduced expression of

PCNT2 in bipolar disorder brain samples. The exact reason for this discrepancy with our results cannot be pointed out now. One possibility might be the difference of methodological procedures. The SMRI data are based on microarray analysis, whereas, our study was carried out with the TaqMan qRT-PCR method. The differences in sample processing might also have affected the results. The SMRI database reports the use of fixed and frozen tissue samples, whereas, we used the extracted RNA samples that were readily available from SMRI. *PCNT2* is reported to have approximately 20 alternate splice forms. Therefore, the probes used for the expression study might also account for the variation in results. However, our results from brain samples were concordant with that from lymphocyte *PCNT2* expression analysis, in which we again observed a significantly higher expression of *PCNT2* in the bipolar group, compared with the control subjects. Thus, we obtained consistent results with RNA samples from two different tissue sources.

Even though we observed an altered expression of *PCNT2* in the bipolar disorder samples, none of the SNPs analyzed in the study showed a significant association with bipolar disorder. The *PCNT2* gene is 121.6 kb long and consists of 47 exons; 433 SNPs are reported in the gene, of which 37 are in the coding region. In our study, we selected only those SNPs that had a MAF $>$ .1 in the Japanese population and those for which TaqMan assays were possible; the 5′ regulatory region and other regulatory elements were not analyzed, thus precluding the definitive exclusion of *PCNT2* as a candidate gene for bipolar disorder. More SNPs in the coding and regulatory regions of the gene have to be analyzed to determine whether the altered expression of the gene can be attributed to *cis*-acting polymorphisms; it might also be possible that the expression of *PCNT2* gene is regulated by additional *trans*-acting factors. In the 21q22.3 region, multiple studies have replicated the positive linkage with bipolar disorder (53–61). In addition, reduced expression of *TRPC7* (transient receptor potential-related channels), also located in this region, has been observed in bipolar disorder-I patients (62).

In conclusion, this is the first report relating *PCNT2* with a psychiatric disorder. Our findings suggest that enhanced expression of *PCNT2* might be implicated in the pathophysiology of bipolar disorder: the levels of *PCNT2* mRNA in lymphocytes might be a useful biological marker of bipolar disorder. Further studies are required as follows: 1) an association study involving more SNPs and using samples of different ethnic origins, and 2) functional studies to elucidate the role of PCNT2 in CNS activities.

Drs. Anitha, Nakamura, and Yamada contributed equally to this work.

This work was supported by a Grant-in-Aid for Scientific Research (B) from the Ministry of Education, Culture, Sports, Science and Technology of Japan. Postmortem brain tissues were donated by the Stanley Medical Research Institute's brain collection, courtesy of Drs. Michael B. Knable, E. Fuller Torrey, Maree J. Webster, Serge Weis, and Robert H. Yolke.

We declare no conflict of interest.

1. Murray CJ, Lopez AD (1997): Global mortality, disability, and the contribution of risk factors: Global Burden of Disease Study. *Lancet* 349:1436–1442.
2. Weissman MM, Bland RC, Canino GJ, Faravelli C, Greenwald S, Hwu HG, *et al.* (1996): Cross-national epidemiology of major depression and bipolar disorder. *JAMA* 276:293–299.
3. Kato T (2001): Molecular genetics of bipolar disorder. *Neurosci Res* 40: 105–113.
4. Blackwood DH, Fordyce A, Walker MT, St Clair DM, Porteous DJ, Muir WJ (2001): Schizophrenia and affective disorders—cosegregation with a translocation at chromosome 1q42 that directly disrupts brain-expressed genes: Clinical and P300 findings in a family. *Am J Hum Genet* 69:428–433.
5. Millar JK, Wilson-Annan JC, Anderson S, Christie S, Taylor MS, Semple CA, *et al.* (2000): Disruption of two novel genes by a translocation co-segregating with schizophrenia. *Hum Mol Genet* 9:1415–1423.
6. Millar JK, Christie S, Anderson S, Lawson D, Hsiao-Wei Loh D, Devon RS, *et al.* (2001): Genomic structure and localisation within a linkage hotspot of Disrupted In Schizophrenia 1, a gene disrupted by a translocation segregating with schizophrenia. *Mol Psychiatry* 6:173–178.
7. St Clair D, Blackwood D, Muir W, Carothers A, Walker M, Spowart G, *et al.* (1990): Association within a family of a balanced autosomal translocation with major mental illness. *Lancet* 336:13–16.
8. Devon RS, Anderson S, Teague PW, Burgess P, Kipari TM, Semple CA, *et al.* (2001): Identification of polymorphisms within Disrupted in Schizophrenia 1 and Disrupted in Schizophrenia 2, and an investigation of their association with schizophrenia and bipolar affective disorder. *Psychiatr Genet* 11:71–78.
9. Callicott JH, Straub RE, Pezawas L, Egan MF, Mattay VS, Hariri AR, *et al.* (2005): Variation in DISC1 affects hippocampal structure and function and increases risk for schizophrenia. *Proc Natl Acad Sci U S A* 102:8627–8632.
10. Hennah W, Varilo T, Kestila M, Paunio T, Arajarvi R, Haukka J, *et al.* (2003): Haplotype transmission analysis provides evidence of association for DISC1 to schizophrenia and suggests sex-dependent effects. *Hum Mol Genet* 12:3151–3159.
11. Kockelkorn TT, Arai M, Matsumoto H, Fukuda N, Yamada K, Minabe Y, *et al.* (2004): Association study of polymorphisms in the 5′ upstream region of human DISC1 gene with schizophrenia. *Neurosci Lett* 368:41–45.
12. Sachs NA, Sawa A, Holmes SE, Ross CA, DeLisi LE, Margolis RL (2005): A frameshift mutation in Disrupted in Schizophrenia 1 in an American family with schizophrenia and schizoaffective disorder. *Mol Psychiatry* 10:758–764.
13. Hodgkinson CA, Goldman D, Jaeger J, Persaud S, Kane JM, Lipsky RH, Malhotra AK (2004): Disrupted in schizophrenia 1 (DISC1): Association with schizophrenia, schizoaffective disorder, and bipolar disorder. *Am J Hum Genet* 75:862–872.
14. Thomson PA, Wray NR, Millar JK, Evans KL, Hellard SL, Condie A, *et al.* (2005): Association between the TRAX/DISC locus and both bipolar disorder and schizophrenia in the Scottish population. *Mol Psychiatry* 10:657–668, 616.
15. Brandon NJ, Handford EJ, Schurov I, Rain JC, Pelling M, Duran-Jimeniz B, *et al.* (2004): Disrupted in Schizophrenia 1 and Nudel form a neurodevelopmentally regulated protein complex: Implications for schizophrenia and other major neurological disorders. *Mol Cell Neurosci* 25:42–55.
16. Ozeki Y, Tomoda T, Kleiderlein J, Kamiya A, Bord L, Fujii K, *et al.* (2003): Disrupted-in-Schizophrenia-1 (DISC-1): Mutant truncation prevents binding to NudE-like (NUDEL) and inhibits neurite outgrowth. *Proc Natl Acad Sci U S A* 100:289–294.
17. Millar JK, Christie S, Porteous DJ (2003): Yeast two-hybrid screens implicate DISC1 in brain development and function. *Biochem Biophys Res Commun* 311:1019–1025.
18. Miyoshi K, Honda A, Baba K, Taniguchi M, Oono K, Fujita T, *et al.* (2003): Disrupted-In-Schizophrenia 1, a candidate gene for schizophrenia, participates in neurite outgrowth. *Mol Psychiatry* 8:685–694.
19. Morris JA, Kandpal G, Ma L, Austin CP (2003): DISC1 (Disrupted-In-Schizophrenia 1) is a centrosome-associated protein that interacts with MAP1A, MIPT3, ATF4/5 and NUDEL: regulation and loss of interaction with mutation. *Hum Mol Genet* 12:1591–1608.
20. Miyoshi K, Asanuma M, Miyazaki I, Diaz-Corrales FJ, Katayama T, Tohyama M, Ogawa N (2004): DISC1 localizes to the centrosome by binding to kendrin. *Biochem Biophys Res Commun* 317:1195–1199.
21. Yamada K, Nakamura K, Minabe Y, Iwayama-Shigeno Y, Takao H, Toyota T, *et al.* (2004): Association analysis of FEZ1 variants with schizophrenia in Japanese cohorts. *Biol Psychiatry* 56:683–690.
22. Baron M (2002): Manic-depression genes and the new millennium: Poised for discovery. *Mol Psychiatry* 7:342–358.
23. Gladkevich A, Kauffman HF, Korf J (2004): Lymphocytes as a neural probe: Potential for studying psychiatric disorders. *Prog Neuropsychopharmacol Biol Psychiatry* 28:559–576.

24. Torrey EF, Webster M, Knable M, Johnston N, Yolken RH (2000): The Stanley foundation brain collection and neuropathology consortium. *Schizophr Res* 44:151–155.
25. American Psychiatric Association (1994): *Diagnostic and Statistical Manual of Mental Disorders, 4th ed.* Washington, DC: American Psychiatric Association.
26. Overall JE, Gorham DR (1962): The brief psychiatric rating scale. *Psychol Rep* 10:799–812.
27. Hamilton M (1960): A rating scale for depression. *J Neurol Neurosurg Psychiatry* 23:56–62.
28. American Psychiatric Association (2000): *Diagnostic and Statistical Manual of Mental Disorders*, 4th ed., *Text Revision*. Washington, DC: American Psychiatric Association.
29. Ranade K, Chang MS, Ting CT, Pei D, Hsiao CF, Olivier M, *et al.* (2001): High-throughput genotyping with single nucleotide polymorphisms. *Genome Res* 11:1262–1268.
30. Dudbridge F (2003): Pedigree disequilibrium tests for multilocus haplotypes. *Genet Epidemiol* 25:115–121.
31. Balczon R, Bao L, Zimmer WE (1994): PCM-1, A 228-kD centrosome autoantigen with a distinct cell cycle distribution. *J Cell Biol* 124:783–793.
32. Chen D, Purohit A, Halilovic E, Doxsey SJ, Newton AC (2004): Centrosomal anchoring of protein kinase C betaII by pericentrin controls microtubule organization, spindle function, and cytokinesis. *J Biol Chem* 279: 4829–4839.
33. Dictenberg JB, Zimmerman W, Sparks CA, Young A, Vidair C, Zheng Y, *et al.* (1998): Pericentrin and gamma-tubulin form a protein complex and are organized into a novel lattice at the centrosome. *J Cell Biol* 141:163–174.
34. Diviani D, Langeberg LK, Doxsey SJ, Scott JD (2000): Pericentrin anchors protein kinase A at the centrosome through a newly identified RII-binding domain. *Curr Biol* 10:417–420.
35. Doxsey SJ, Stein P, Evans L, Calarco PD, Kirschner M (1994): Pericentrin, a highly conserved centrosome protein involved in microtubule organization. *Cell* 76:639–650.
36. Kubo A, Sasaki H, Yuba-Kubo A, Tsukita S, Shiina N (1999): Centriolar satellites: Molecular characterization, ATP-dependent movement toward centrioles and possible involvement in ciliogenesis. *J Cell Biol* 147:969–980.
37. Rempel N (2001): Centrosomes as scaffolds: The role of pericentrin and protein kinase A-anchoring proteins. *Einstein Quart J Biol and Med* 18: 54–58.
38. Zimmerman WC, Sillibourne J, Rosa J, Doxsey SJ (2004): Mitosis-specific anchoring of gamma tubulin complexes by pericentrin controls spindle organization and mitotic entry. *Mol Biol Cell* 15:3642–3657.
39. Benes FM, Vincent SL, Todtenkopf M (2001): The density of pyramidal and nonpyramidal neurons in anterior cingulate cortex of schizophrenic and bipolar subjects. *Biol Psychiatry* 50:395–406.
40. Benes FM, Walsh J, Bhattacharyya S, Sheth A, Berretta S (2003): DNA fragmentation decreased in schizophrenia but not bipolar disorder. *Arch Gen Psychiatry* 60:359–364.
41. Harrison PJ (2002): The neuropathology of primary mood disorder. *Brain* 125:1428–1449.
42. Benes FM (2004): The role of apoptosis in neuronal pathology in schizophrenia and bipolar disorder. *Curr Opin Psychiatry* 17:189–190.
43. Beyer JL, Krishnan KR (2002): Volumetric brain imaging findings in mood disorders. *Bipolar Disord* 4:89–104.
44. Soares JC (2003): Contributions from brain imaging to the elucidation of pathophysiology of bipolar disorder. *Int J Neuropsychopharmacol* 6:171–180.
45. Soares JC, Mann JJ (1997): The functional neuroanatomy of mood disorders. *J Psychiatr Res* 31:393–432.
46. Blumberg HP, Kaufman J, Martin A, Charney DS, Krystal JH, Peterson BS (2004): Significance of adolescent neurodevelopment for the neural circuitry of bipolar disorder. *Ann N Y Acad Sci* 1021:376–383.
47. Cannon M, Caspi A, Moffitt TE, Harrington H, Taylor A, Murray RM, Poulton R (2002): Evidence for early-childhood, pan-developmental impairment specific to schizophreniform disorder: Results from a longitudinal birth cohort. *Arch Gen Psychiatry* 59:449–456.
48. Chen BK, Sassi R, Axelson D, Hatch JP, Sanches M, Nicoletti M, *et al.* (2004): Cross-sectional study of abnormal amygdala development in adolescents and young adults with bipolar disorder. *Biol Psychiatry* 56: 399–405.
49. Crow TJ (1995): Constraints on concepts of pathogenesis. Language and the speciation process as the key to the etiology of schizophrenia. *Arch Gen Psychiatry* 52:1011–1014; discussion 1019–1024.
50. David AS, Malmberg A, Brandt L, Allebeck P, Lewis G (1997): IQ and risk for schizophrenia: A population-based cohort study. *Psychol Med* 27: 1311–1323.
51. Harwood AJ (2003): Neurodevelopment and mood stabilizers. *Curr Mol Med* 3:472–482.
52. van Os J, Jones P, Lewis G, Wadsworth M, Murray R (1997): Developmental precursors of affective illness in a general population birth cohort. *Arch Gen Psychiatry* 54:625–631.
53. Aita VM, Liu J, Knowles JA, Terwilliger JD, Baltazar R, Grunn A, *et al.* (1999): A comprehensive linkage analysis of chromosome 21q22 supports prior evidence for a putative bipolar affective disorder locus. *Am J Hum Genet* 64:210–217.
54. Alda M (1999): Pharmacogenetics of lithium response in bipolar disorder. *J Psychiatry Neurosci* 24:154–158.
55. Detera-Wadleigh SD, Badner JA, Goldin LR, Berrettini WH, Sanders AR, Rollins DY, *et al.* (1996): Affected-sib-pair analyses reveal support of prior evidence for a susceptibility locus for bipolar disorder, on 21q. *Am J Hum Genet* 58:1279–1285.
56. Detera-Wadleigh SD, Badner JA, Yoshikawa T, Sanders AR, Goldin LR, Turner G, *et al.* (1997): Initial genome scan of the NIMH genetics initiative bipolar pedigrees: Chromosomes 4, 7, 9, 18, 19, 20, and 21q. *Am J Med Genet* 74:254–262.
57. Kaneva RP, Chorbov VM, Milanova VK, Kostov CS, Nickolov KI, Chakarova CF, *et al.* (2004): Linkage analysis in bipolar pedigrees adds support for a susceptibility locus on 21q22. *Psychiatr Genet* 14:101–106.
58. Kwok JB, Adams LJ, Salmon JA, Donald JA, Mitchell PB, Schofield PR (1999): Nonparametric simulation-based statistical analyses for bipolar affective disorder locus on chromosome 21q22.3. *Am J Med Genet* 88: 99–102.
59. Liu J, Juo SH, Terwilliger JD, Grunn A, Tong X, Brito M, *et al.* (2001): A follow-up linkage study supports evidence for a bipolar affective disorder locus on chromosome 21q22. *Am J Med Genet* 105:189–194.
60. Smyth C, Kalsi G, Curtis D, Brynjolfsson J, O'Neill J, Rifkin L, *et al.* (1997): Two-locus admixture linkage analysis of bipolar and unipolar affective disorder supports the presence of susceptibility loci on chromosomes 11p15 and 21q22. *Genomics* 39:271–278.
61. Straub RE, Lehner T, Luo Y, Loth JE, Shao W, Sharpe L, *et al.* (1994): A possible vulnerability locus for bipolar affective disorder on chromosome 21q22.3. *Nat Genet* 8:291–296.
62. Yoon IS, Li PP, Siu KP, Kennedy JL, Macciardi F, Cooke RG, *et al.* (2001): Altered TRPC7 gene expression in bipolar-I disorder. *Biol Psychiatry* 50: 620–626.